Computers & Industrial Engineering 168 (2022) 108113

Contents lists available at ScienceDirect

Computers & Industrial Engineering

journal homepage: www.elsevier.com/locate/caie

Real-time train regulation method for metro lines with substation peak power reduction

Bo Jin, Xiaoyun Feng, Qingyuan Wang, Pengfei Sun *

School of Electrical Engineering, Southwest Jiaotong University, Chengdu 611756, China

ARTICLE INFO

Keywords:
Urban rail transit
Timetable rescheduling
Model predictive control
Mixed integer quadratic programming

ABSTRACT

In high-frequency metro lines, train delays and substation peak power often occur, affecting safe and efficient train operation. In this paper, we propose real-time train regulation methods considering substation peak power reduction, in which runtimes and dwelltimes are adjusted to minimize the timetable and headway deviations and avoid multiple train accelerating. Firstly, we proposed two indirect indicators, i.e. overlapping time between accelerating phases and overlapping quantity between accelerating phases, which are minimized to suppress substation peak power in joint optimal train regulation models. The joint optimal train regulation models are based on the traditional real-time train regulation model considering the train traffic dynamics and control constraints. For the real-time requirement of train regulation, model predictive control (MPC) algorithms are designed to solve the formulated joint optimal control models, which generate the optimal train regulation strategies at each control cycle based on the real-time updated feedback system states. Finally, numerical examples based on one of the Guangzhou metro lines are implemented to verify the effectiveness and robustness of the proposed methods. The results show that the train regulation strategy with minimizing the overlapping quantity can not only suppress train delays and substation peak power, but also meet the real-time computation requirement.

1. Introduction

Urban rail transit (URT) systems play an important role in urban public transportation, especially in big cities (e.g. Tokyo, Paris, and Beijing). Trains in URT systems are keeping high-frequency to meet large passenger transportation demands. However, due to the high-frequency operation and crowded environments, perturbances often occur in URT systems, which will cause train delays. If the train delays cannot be suppressed in time, they will spread to subsequent trains and stations. In addition, the train delays will affect the quality of service and even cause system interruptions (Yin, Tang, Yang, Gao, & Ran, 2016).

To suppress the train delays, train regulation strategies are applied to adjust disturbed timetables. Arrival and departure times are adjusted under small perturbances (i.e. disturbances), and the plan of train services is also adjusted under big perturbances (i.e. disruptions) (Hong et al., 2021). Minimizing timetable deviation and headway deviation are two main goals of train regulation, in which the first term is used for improving the commercial speed and the second term is used to improve the regularity of headway (Zhang, Li, & Yang, 2019). In addition, considering the issue of environmental sustainability, energy-saving is also considered in the train regulation strategy (Lin & Sheu, 2011; Sheu & Lin, 2012).

On the other hand, the high substation peak power is also a major problem in high-frequency URT systems, which affect the safe and efficient operation of trains. Although, some researches in literature (Bärmann, Martin, & Schneider, 2021; Chen, Lin, & Liu, 2005; Jin, Feng, Wang, Sun, & Fang, 2021) begin to stress this problem, in which timetables are optimized to suppress peak power in scheduling processes. To the best of our knowledge, there is no train regulation study combining substation peak power reduction. Based on this, the aim of this paper is to determine the train regulation strategy considering suppressing the substation peak power, so as to ensure the stability of URT systems.

1.1. Literature review

The train regulation problem for URT systems is usually formulated as an optimization problem and solved by different algorithms. Pellegrini, Marlière, Pesenti, and Rodriguez (2015), Pellegrini, Pesenti, and

* Corresponding author.
E-mail address: pengfeisun@swjtu.edu.cn (P. Sun).

https://doi.org/10.1016/j.cie.2022.108113
Received 19 June 2021; Received in revised form 15 March 2022; Accepted 16 March 2022
Available online 23 March 2022

Rodriguez (2019) formulated the train regulation problem into a mixed integer linear programming model and designed a heuristic algorithm to find the optimal train rescheduling plans. Schön and König (2018) presented a multi-stage stochastic dynamic programming model for the train regulation problem, in which uncertainties over future delays were considered. Based on the alternative graph method, Ariano, Corman, Pacciarelli, and Pranzo (2008) described the train regulation problem as a job shop scheduling problem. They made use of a branch-and-bound algorithm for sequencing train movements and developed a local search algorithm for train rerouting optimization purposes. In addition, tabu search algorithm (Corman, D'Ariano, Pacciarelli, & Pranzo, 2010), heuristic algorithm (Corman, D'Ariano, Pacciarelli, & Pranzo, 2012) and variable neighbourhood search algorithm (Samà, D'Ariano, Corman, & Pacciarelli, 2017) were applied to solve the train regulation problem based on the alternative graph method, aiming to reduce computation cost. For achieving real-time application of train regulation strategies, Šemrov, Marsetič, Žura, Todorovski, and Srdic (2016) introduced a train regulation method based on reinforcement learning to reduce computation time. Wang et al. (2021) developed a two-stage approach to enhance computational efficiency, where a small-size optimization problem was solved in the first stage and a mixed integer linear programming problem was solved in the second stage according to the first stage solution. Li, Li, Liu, Gao, and Yang (2021) proposed a decomposition method based on the alternating direction method of multipliers to divide the train regulation problem into many sub-problems, one for each train. Each sub-problem could be computed in a distributed manner to realize real-time control.

Based on the discrete-event traffic model, some studies solved the real-time train regulation problem based on model predictive control (MPC). MPC is a model-based closed-loop control framework that adopts a strategy of rolling optimization and thus repeatedly optimizes control actions in real-time, which not only reduces the computation cost but also improve the robustness of control actions (Zhang, Li, Wang, Wang, & Yang, 2021). MPC has been widely applied in transportation systems for trajectory following (Wang, Zha, & Wang, 2021), energy management (Novak, Lesic, & Vasak, 2018), and traffic control (Sirmatel & Geroliminis, 2021; Wu, Li, Xi, & De Schutter, 2021). More details about the application of MPC in engineering fields can be seen in the study (Schwenzer, Ay, Bergs, & Abel, 2021). For the train regulation problem, Campion, Van Breusegem, Pinson, and Bastin (1985) proposed a state-space model to describe the traffic dynamics, and set minimizing the timetable and headway deviations as the model objectives. They applied the one-step optimal control to achieve real-time state feedback control. Breusegem, Campion, and Bastin,. (1991) established a discrete-event traffic model of metro lines and designed a state feedback control algorithm to ensure system stability. This model was useful to analyze the stability of the URT train regulation problem. Grube and Cipriano (2010) presented a novel strategy based on MPC for real-time control of URT systems. The strategy was computed using genetic algorithms at each control cycle. Wang, Li, Su, and Tang (2019) designed a fuzzy predictive controller to reduce train delays considering fuzzy passenger arrival rate. Moaveni and Najafi (2018) designed a robust MPC algorithm to compensate the disturbances and to regulate traffic in the presence of operational constraints, in which an uncertain model is considered to accommodate variation in passenger demand. Wang, Zhu, Li, Yang, and De Schutter (2022) proposed a novel two-layer hierarchical model predictive control method combining train regulation and train control for minimizing train delays and cancellations. By applying MPC, the original train regulation optimization problem could be split into a set of convex quadratic programming problems, which could be calculated efficiently and satisfied the real-time control requirement (Li, Yang, & Gao, 2019).

In the optimal train regulation problem, minimizing the impact of disturbances is the main optimization goal, and energy-saving rescheduling is also a hot topic in recent years (Li et al., 2020). Lin and Sheu (2011) built a traffic-energy model to characterize the complicated dynamics with regard to the traffic and the energy consumption of train running processes. They designed an adaptive-optimal-control algorithm to optimize train regulation strategies through reinforcement learning. Sheu and Lin (2012) proposed a dual heuristic programming to obtain the energy-saving train regulation strategy via station dwell time adjusting and running process coasting control. Yin et al. (2016) established a stochastic model jointly considering the time delay of affected passengers, passenger total traveling time and operational costs of trains, which was solved by an approximate dynamic programming approach within a short computation time. Zhang et al. (2019) combined minimizing the energy consumption into the objective function of the train regulation problem, and designed a MPC algorithm to obtain optimal train regulation strategies in real-time.

On the other hand, reducing substation peak power has been considered in the train timetable optimization problem, which keeps the safe and efficient operation of trains. Chen et al. (2005) built a timetable optimization model to avoid simultaneous accelerating of multiple trains, aiming to reduce maximum traction power, which was solved by genetic algorithms. Jin et al. (2021) transformed the timetable optimization model considering peak power reduction into a mixed integer programming model, which could only be solved offline due to its complexity. Bärmann et al. (2021) proposed a specially tailored exact Benders algorithm to calculate an optimal timetable with less simultaneous train accelerating, so as to limit peak consumption and improve the stability of substations. However, there is no work considering reducing peak power in the train regulation problem.

1.2. Proposed approach and contributions

As shown above, a variety of studies have focused on the train regulation problem, part of them establish complicated optimization models considering multiple optimization goals, like minimizing timetable deviation, minimizing headway deviation, and energy-saving. Meanwhile, many of them propose novel algorithms to obtain the optimal train regulation strategy within a short computation time aiming to achieve real-time control. This paper focuses on employing the MPC algorithm to the train regulation problem under small perturbations (disturbances) for metro lines, in which substation peak power is reduced by avoiding simultaneous train acceleration. Although studies (Bärmann et al., 2021; Chen et al., 2005; Jin et al., 2021) have stressed reducing substation peak power in the timetable optimization problem, the proposed offline optimization methods are not suitable for applying to the real-time train regulation problem. Specifically, we aim to make the following contributions to the study of the train regulation problem.

(1) Train regulation models, which consider train traffic dynamics and substation peak power, are formulated. Two indirect indicators (i.e. overlapping time between accelerating phases, overlapping quantity between accelerating phases) are introduced to express the substation peak power, which are minimized to reduce peak power. In addition, the proposed models are rebuilt into MIQP problems for better solving.

(2) MPC algorithms are developed to produce the optimal train regulation strategies reducing the influence of disturbances and substation peak power in real-time. By applying MPC, the complex MIQP problems are divided into a set of simple MIQP problems. At each control cycle, optimal control actions are obtained by effectively solving these subproblems, which satisfies the real-time control requirement.

The rest of this paper is organized as follows. In Section 2, we give a description of the metro train regulation problems considering substation peak power reduction in an open metro line. Then, we propose the solution methodology for the metro train regulation problems based on MPC in Section 3. In Section 4, we give numerical examples based on one of the Guangzhou metro lines, to demonstrate the effectiveness and robustness of the proposed approaches. We conclude this paper in Section 5.

2. Problem description

In this paper, we consider a metro line with $2I$ stations, where J trains orderly run through stations, as shown in Fig. 1.

2.1. Notations and parameters

For modelling convenience, Table 1 firstly gives all the relevant notations and parameters used in this paper.

2.2. Traditional train regulation model

2.2.1. Train traffic dynamics model

Based on the discrete-event model proposed by V.V. Breusegem et al. (1991), the train traffic dynamics model is formulated. The train traffic dynamics for the actual departure time of train j at station $i+1$ can be described as:

$$t_{i+1}^j = t_i^j + r_i^j + d_{i+1}^j \tag{1}$$

which is actually the actual departure time of train j at station i plus the actual runtime from station i to station $i+1$ and the actual dwelltime at station $i+1$.

The actual runtime of train j from station i to station $i+1$ can be described as:

$$r_i^j = R_i + ur_i^j + wr_i^j \tag{2}$$

which is usually affected by uncertain runtime disturbance wr_i^j, and control action ur_i^j is applied to reduce the effect of the disturbance.

Meanwhile, the actual dwelltime of train j at station $i+1$ is affected by uncertain dwelltime disturbance wd_{i+1}^j, and control action ud_i^j is applied:

$$d_{i+1}^j = D_{i+1} + ud_{i+1}^j + wd_{i+1}^j \tag{3}$$

In addition, by combining Eq. 1–3, the train traffic dynamics model can be described as:

$$t_{i+1}^j = t_i^j + R_i + D_{i+1} + ur_i^j + ud_{i+1}^j + wr_i^j + wd_{i+1}^j \tag{4}$$

Besides, let k represent the stage, the actual departure time at stage k is described as the matrix form $t_k = [t_1^{k-1}, t_2^{k-2}, \ldots, t_I^{k-I}]^T$ (Li, Dessouky, Yang, & Gao, 2017; Wang, Li, Tang, & Yang, 2022), which denotes the departure times of trains at all the stations. Based on Eq. 4, the matrix form of the train traffic dynamics model in the up direction can be described as:

$$t_{k+1} = \Lambda t_k + T_{0,k} + R + D + ur_k + ud_k + wr_k + wd_k \tag{5}$$

where, $ur_k = [ur_0^k, ur_1^{k-1}, \ldots, ur_{I-1}^{k-I+1}]^T$, $ur_0^k = 0$; $ud_k = [ud_1^k, ud_2^{k-1}, \ldots, ud_I^{k-I+1}]^T$; $wr_k = [wr_0^k, wr_1^{k-1}, \ldots, wr_{I-1}^{k-I+1}]^T$, $wr_0^k = 0$; $wd_k = [wd_1^k, wd_2^{k-1}, \ldots, wd_I^{k-I+1}]^T$; $R = [R_0, R_1, \ldots, R_{I-1}]^T$, $R_0 = 0$; $D = [D_1, D_2, \ldots, D_I]^T$; $\Lambda = [\Lambda_{ij}]_{I\times I}$, with $\Lambda_{ij} = 1$ for $i = j+1$ and $\Lambda_{ij} = 0$ otherwise; $T_{0,k} = [Ta_1^k, 0, \ldots, 0]_{1\times I}^T$, Ta_1^k is the departure time of train k at station 1, $Ta_1^{k+1} = Ta_1^k + H$. To better illustrate the variation of the state variable in Eq. 5, the illustration of the transfer from stage k to stage $k+1$ is shown in Fig. 2. Control actions ur_k and ud_k are applied to suppress the influence of deviations wr_k and wd_k at stage k.

Table 1
Notations and parameters.

Index	Description
i	Index of stations, $1 \leqslant i \leqslant 2I$, $[1, \ldots, I]$ for the up direction and $[I+1, \ldots, 2I]$ for the down direction
j	Index of trains, $1 \leqslant j \leqslant J$
Parameters	**Description**
T_i^j	Nominal departure time of train j at station i
$\Psi_{i,min}$	Minimum departure-arrival interval at station i
D_i	Nominal dwelltime at station i
$D_{i,min}$	Minimal dwelltime at station i
H	Nominal headway
R_i	Nominal runtime from station i to station $i+1$
$R_{i,min}$	Minimum runtime from station i to station $i+1$
A_i	Accelerating duration from station i to station $i+1$
State variables	**Description**
t_i^j	Actual departure time of train j at station i
d_i^j	Actual dwelltime of train j at station i
r_i^j	Actual runtime of train j from station i to station $i+1$
x_i^j	Deviation of train j from nominal departure time at station i
o_i^j	Overlapping time between train j leaving station i and train $j-1$ leaving station $i+1$
wd_i^j	Disturbance of dwelltime of train j at station i
wr_i^j	Disturbance of runtime of train j from station i to station $i+1$
Decision variables	**Description**
ud_i^j	Control action of dwelltime of train j at station i
ur_i^j	Control action of runtime of train j from station i to station $i+1$

2.2.2. Objective functions

The objectives of the traditional train regulation problem for metro lines is to minimize the timetable deviation, headway deviation and magnitude of the control actions (Zhang et al., 2019), which can be described as:

$$J = p_1 \sum_{i,j} (x_i^j)^2 + p_2 \sum_{i,j} (x_i^j - x_i^{j-1})^2 + p_3 \sum_{i,j} (ur_i^j)^2 + p_3 \sum_{i,j} (ud_i^j)^2 \tag{6}$$

where, p_1, p_2 and p_3 are the weight coefficients.

The first part in the objective function 6 represents the sum of timetable deviation, which is reduced to suppress delay propagation. The actual departure times will deviate from the nominal scheduling due to disturbances. The deviation from the nominal timetable of train j at station $i+1$ can be defined as:

$$x_{i+1}^j = t_{i+1}^j - T_{i+1}^j \tag{7}$$

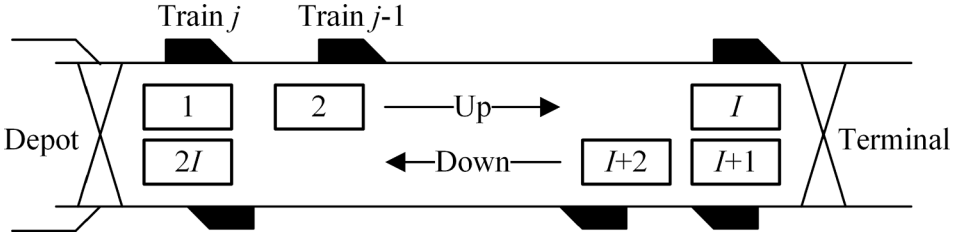

Fig. 1. The illustration of the metro line.

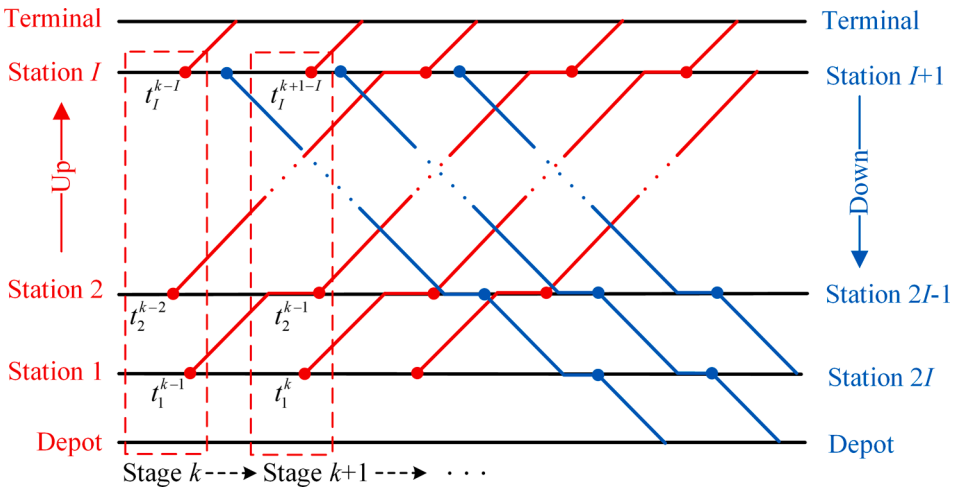

Fig. 2. The illustration of the transfer from stage k to stage $k+1$.

which can be rewritten as the following vector and matrix form:

$$x_{k+1} = t_{k+1} - T_{k+1} \tag{8}$$

where, $x_k = [x_1^{k-1}, x_2^{k-2}, \ldots, x_I^{k-I}]^T$; $T_k = [T_1^{k-1}, T_2^{k-2}, \ldots, T_I^{k-I}]^T$.

The second part in the objective function 6 represents the sum of headway deviation, which is minimized to keep the regularity of headway and thus reduce passenger waiting time. The headway between train j and train $j-1$ at station i also deviates from the nominal headway H, which can be defined as:

$$(t_{i+1}^j - t_{i+1}^{j-1}) - H = x_{i+1}^j - x_{i+1}^{j-1} \tag{9}$$

The third and fourth parts in the objective function 6 represent the sum of the magnitude of control actions, which is minimized to penalize the large control actions.

In addition, the objective function 6 can be rewritten with the vector and matrix form as:

$$J_k = p_1 x_{k+1}^T x_{k+1} + p_2 (x_{k+1} - x_k)^T (x_{k+1} - x_k) + p_3 ur_k^T ur_k + p_3 ud_k^T ud_k \tag{10}$$

2.2.3. System constraints

To ensure the safe and feasible operation of the train regulation strategy, the following constraints should be considered.

Safety constraint. To keep the safety interval between the arrival time of train j and the departure time of train $j-1$ at station i:

$$t_i^j - d_i^j - t_i^{j-1} \geqslant \Psi_{i,min} \tag{11}$$

Dwelltime constraint. To ensure the dwelltime at each station is feasible in practice operation, which should be larger than the minimum dwelltime:

$$D_i + ud_i^j + \omega d_i^j \geqslant D_{i,min} \tag{12}$$

Runtime constraint. To ensure the runtime at each section is feasible in practice operation, which should be larger than the minimum runtime:

$$R_i + ur_i^j + \omega r_i^j \geqslant R_{i,min} \tag{13}$$

Control constraint. For the practical limits for the control input, the following control constraint is considered to ensure the control actions in acceptable extents:

$$\begin{cases} UR_{i,min} \leqslant ur_i^j \leqslant UR_{i,max} \\ UD_{i,min} \leqslant ud_i^j \leqslant UD_{i,max} \end{cases} \tag{14}$$

where, $UR_{i,min}$ and $UR_{i,max}$ are the lower and upper limitations of the runtime control action from station i to station $i+1$; $UD_{i,min}$ and $UD_{i,max}$ are the lower and upper limitations of the dwelltime control action at station i.

In addition, the above system constraints can be rewritten with the vector and matrix form as:

$$\begin{cases} t_{k+1} - D - ud_k - \omega d_k - t_k \geqslant \Psi_{min} \\ D + ud_k + \omega d_k \geqslant D_{min} \\ R + ur_k + \omega r_k \geqslant R_{min} \\ UR_{min} \leqslant ur_k \leqslant UR_{max} \\ UD_{min} \leqslant ud_k \leqslant UD_{max} \end{cases} \tag{15}$$

where, $\Psi_{min} = [\Psi_{1,min}, \Psi_{2,min}, \cdots, \Psi_{I,min}]^T$;
$D_{min} = [D_{1,min}, D_{2,min}, \cdots, D_{I,min}]^T$;
$R_{min} = [R_{0,min}, R_{1,min}, \cdots, R_{I-1,min}]^T, R_{0,min} = 0$;
$UR_{min} = [UR_{0,min}, UR_{1,min}, \cdots, UR_{I-1,min}]^T$;
$UR_{max} = [UR_{0,max}, UR_{1,max}, \cdots, UR_{I-1,max}]^T$;
$UD_{min} = [UD_{1,min}, UD_{2,min}, \cdots, UD_{I,min}]^T$;
$UD_{max} = [UD_{1,max}, UD_{2,max}, \cdots, UD_{I,max}]^T$.

2.2.4. Optimal control problem

Given the train traffic dynamics, by considering the objective function and system constraints, the train regulation problem can be formulated as the following optimal control problem:

$$\begin{cases} \min \quad \sum_{k=j_0}^{j_f} \{p_1 x_{k+1}^T x_{k+1} + p_2 (x_{k+1} - x_k)^T (x_{k+1} - x_k) + p_3 ur_k^T ur_k \\ \qquad\qquad + p_3 ud_k^T ud_k\} \\ \text{s.t.} \quad t_{k+1} = \Lambda t_k + T_{0,k} + R + ur_k + \omega r_k + D + ud_k + \omega d_k \\ \qquad x_{k+1} = t_{k+1} - T_{k+1} \\ \qquad \Psi_{min} \leqslant t_{k+1} - D - ud_k - \omega d_k - t_k \\ \qquad D_{min} \leqslant D + ud_k + \omega d_k \\ \qquad R_{min} \leqslant R + ur_k + \omega r_k \\ \qquad UR_{min} \leqslant ur_k \leqslant UR_{max} \\ \qquad UD_{min} \leqslant ud_k \leqslant UD_{max} \\ \qquad \text{for } k \in \{j_0, \ldots, j_f\}. \end{cases} \tag{16}$$

where, j_0 is the initial state number; j_f is the terminal state number. Similarly, the traditional train regulation model in the down direction can be built in the same way with $i \in \{I+1, I+2, \ldots, 2I\}$.

2.3. Train regulation model with minimizing overlapping time

2.3.1. Overlapping time between accelerating phases

In real-world operation, an extreme high substation power occurs if numerous adjacent trains are accelerating simultaneously (Chen et al., 2005). Considering the up and down directions, the adjacent trains mean trains departing from adjacent stations in the same direction and trains departing from the same station in the opposite direction. In this paper, the overlapping time between accelerating phases is taken as an indirect evaluation of substation peak power. In previous studies, the overlapping time between accelerating and braking phases is maximized to overlap the train accelerating and braking phases (Ning, Zhou, Long, & Tao, 2018; Yang, Li, Gao, Wang, & Tang, 2013). In this paper, the overlapping time between accelerating phases is minimized to avoid overlapping of accelerating phases. As shown in Fig. 3, when trains accelerate at the same time, the accelerating phases of trains will overlap. The simultaneous accelerating of trains can be suppressed by minimizing the overlapping time between accelerating phases, thus to reduce substation peak power. Based on the calculation of the overlapping time between accelerating and braking phases (Ramos, Pena, & Fernandez, 2007), the model to calculate the overlapping time between accelerating phases is built in this section.

Let A_i be the train accelerating duration from station i to station $i+1$, then $t_i^j+A_i$ is defined as the end of the accelerating phase of train i after leaving station j. The overlapping time between train j leaving station i and train $j-1$ leaving station $i+1$ can be divided into six conditions as shown in Table 2. For example, as shown in Fig. 3 (a), $t_i^j \leqslant t_{i+1}^{j-1}, t_{i+1}^{j-1} \leqslant t_i^j + A_i$ and $t_i^j + A_i \leqslant t_{i+1}^{j-1} + A_{i+1}$, then the overlapping time is equal to $t_i^j + A_i - t_{i+1}^{j-1}$, which corresponds to Case 5. Similarly, the overlapping time between train j leaving station i and train $2I-j+1$ leaving station $2I-i+1$ (the same station of station i) can also be divided into six conditions. In this section, the overlapping time between train j leaving station i and train $j-1$ leaving station $i+1$ is taken as an example to explain the calculation of overlapping time.

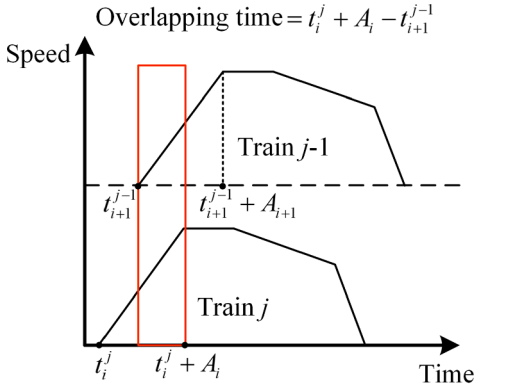

(a) adjacent trains in the same direction

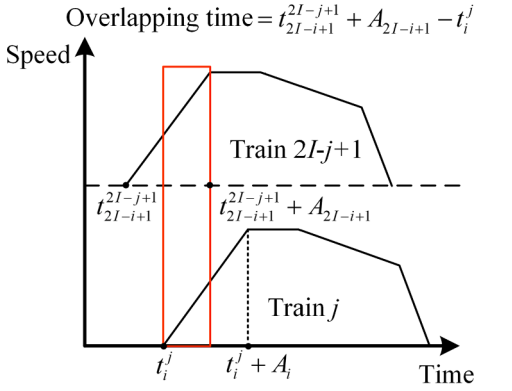

(b) adjacent trains in the opposite direction

Fig. 3. The illustration of the overlapping time between accelerating phases.

Table 2
Six conditions of the overlapping time.

Case	Condition	Overlapping time	$[\eta_{i,1}^j, \eta_{i,2}^j, \eta_{i,3}^j, \eta_{i,4}^j]$
1	$t_i^j \leqslant t_i^j + A_i \leqslant t_{i+1}^{j-1} \leqslant t_{i+1}^{j-1} + A_{i+1}$	0	[1,1,1,1]
2	$t_{i+1}^{j-1} \leqslant t_{i+1}^{j-1} + A_{i+1} < t_i^j \leqslant t_i^j + A_i$	0	[0,0,0,0]
3	$t_{i+1}^{j-1} < t_i^j \leqslant t_i^j + A_i \leqslant t_{i+1}^{j-1} + A_{i+1}$	A_i	[0,1,0,1]
4	$t_i^j \leqslant t_{i+1}^{j-1} \leqslant t_{i+1}^{j-1} + A_{i+1} < t_i^j + A_i$	A_{i+1}	[1,1,0,0]
5	$t_i^j \leqslant t_{i+1}^{j-1} < t_i^j + A_i \leqslant t_{i+1}^{j-1} + A_{i+1}$	$t_i^j + A_i - t_{i+1}^{j-1}$	[1,1,0,1]
6	$t_{i+1}^{j-1} < t_i^j \leqslant t_{i+1}^{j-1} + A_{i+1} < t_i^j + A_i$	$t_{i+1}^{j-1} + A_{i+1} - t_i^j$	[0,1,0,0]

2.3.2. Computation of overlapping time between accelerating phases

In order to distinguish these six conditions, four binary variables ($\eta_{i,1}^j, \eta_{i,2}^j, \eta_{i,3}^j$ and $\eta_{i,4}^j$) are introduced, which are defined as:

$$\begin{cases} t_i^j \leqslant t_{i+1}^{j-1} \Leftrightarrow \eta_{i,1}^j = 1 \\ t_i^j \leqslant t_{i+1}^{j-1} + A_{i+1} \Leftrightarrow \eta_{i,2}^j = 1 \\ t_i^j + A_i \leqslant t_{i+1}^{j-1} \Leftrightarrow \eta_{i,3}^j = 1 \\ t_i^j + A_i \leqslant t_{i+1}^{j-1} + A_{i+1} \Leftrightarrow \eta_{i,4}^j = 1 \end{cases} \tag{17}$$

Then, the relationship between the beginning and the end of accelerating phases can be expressed by these binary variables, as shown in Table 2. For example, when $t_i^j \leqslant t_i^j + A_i \leqslant t_{i+1}^{j-1} \leqslant t_{i+1}^{j-1} + A_{i+1}, [\eta_1, \eta_2, \eta_3, \eta_4] = [1,1,1,1]$, and the overlap time is equal to zero corresponding to Case 1. In addition, based on the Transformation Property 1 in Appendix A, the implication of binary variables 17 can be modelled by the following linear constraints:

$$\begin{cases} t_i^j - t_{i+1}^{j-1} \leqslant \widetilde{M}(1-\eta_{i,1}^j) \\ t_i^j - t_{i+1}^{j-1} \geqslant \varepsilon + (\widetilde{m}-\varepsilon)\eta_{i,1}^j \\ t_i^j - t_{i+1}^{j-1} - A_{i+1} \leqslant \widetilde{M}(1-\eta_{i,2}^j) \\ t_i^j - t_{i+1}^{j-1} - A_{i+1} \geqslant \varepsilon + (\widetilde{m}-\varepsilon)\eta_{i,2}^j \\ t_i^j + A_i - t_{i+1}^{j-1} \leqslant \widetilde{M}(1-\eta_{i,3}^j) \\ t_i^j + A_i - t_{i+1}^{j-1} \geqslant \varepsilon + (\widetilde{m}-\varepsilon)\eta_{i,3}^j \\ t_i^j + A_i - t_{i+1}^{j-1} - A_{i+1} \leqslant \widetilde{M}(1-\eta_{i,4}^j) \\ t_i^j + A_i - t_{i+1}^{j-1} - A_{i+1} \geqslant \varepsilon + (\widetilde{m}-\varepsilon)\eta_{i,4}^j \end{cases} \tag{18}$$

where, ε is a small positive number to transform a strict inequality into an inequality.

In particular, there is no concurrence when a train begins the accelerating phase after the end of the accelerating phase of another train (Case 1: $t_i^j + A_i \leqslant t_{i+1}^{j-1}$ or Case 2: $t_{i+1}^{j-1} + A_{i+1} < t_i^j$), otherwise there is concurrence. To describe this condition, a binary variable $\delta_{i,1}^j$ is introduced:

$$(t_i^j \leqslant t_{i+1}^{j-1} + A_{i+1} \wedge t_i^j + A_i > t_{i+1}^{j-1}) \Leftrightarrow (\eta_{i,2}^j = 1 \wedge \eta_{i,3}^j = 0) \Leftrightarrow (\delta_{i,1}^j = 1) \tag{19}$$

where, $\delta_{i,1}^j = 1$ means there is concurrence, $\delta_{i,1}^j = 0$ means there is no concurrence. According to the relationship between $\eta_{i,2}^j, \eta_{i,3}^j$ and $\delta_{i,1}^j$ in the Eq. 19, $\delta_{i,1}^j$ can be described as:

$$\delta_{i,1}^j = \eta_{i,2}^j (1 - \eta_{i,3}^j) \tag{20}$$

In addition, based on the Transformation Property 2 in Appendix A, the implication of binary variables $\delta_{i,1}^j$ can be modelled by the following linear constraints:

$$\begin{cases} \delta_{i,1}^j \geqslant \eta_{i,2}^j - \eta_{i,3}^j \\ \delta_{i,1}^j \leqslant \eta_{i,2}^j \\ \delta_{i,1}^j \leqslant 1 - \eta_{i,3}^j \end{cases} \tag{21}$$

Then, the overlapping time o_i^j can be described as:

$$\begin{cases} 0 \leqslant o_i^j \\ \widetilde{M}(\delta_{i,1}^j - 1) + [\min(t_i^j + A_i, t_{i+1}^{j-1} + A_{i+1}) - \max(t_i^j, t_{i+1}^{j-1})] \leqslant o_i^j \end{cases} \tag{22}$$

Considering minimizing the overlapping time, when $\delta_{i,1}^j = 1$, the second part of the above equation acts as the only effectual constraint and the value of overlapping time is depended on $[\min(t_i^j + A_i, t_{i+1}^{j-1} + A_{i+1}) - \max(t_i^j, t_{i+1}^{j-1})]$ corresponding to Case 3 to 6, where $\max(t_i^j, t_{i+1}^{j-1})$ represents the beginning of the concurrence and $\min(t_i^j + A_i, t_{i+1}^{j-1} + A_{i+1})$ represents the end of the concurrence. On the other hand, when $\delta_{i,1}^j = 0$, the left side of the second part of the above equation ($-M + [\min(t_i^j + A_i, t_{i+1}^{j-1} + A_{i+1}) - \max(t_i^j, t_{i+1}^{j-1})]$) is negative, and the first part acts as the only effectual constraint, then $o_i^j = 0$ corresponding to Case 1 and 2.

In addition, to define $\max(t_i^j, t_{i+1}^{j-1})$ and $\min(t_i^j + A_i, t_{i+1}^{j-1} + A_{i+1})$, the following binary variables ($\delta_{i,2}^j, \delta_{i,3}^j, \delta_{i,4}^j$ and $\delta_{i,5}^j$) are introduced:

$$\begin{cases} \delta_{i,2}^j = (1 - \eta_{i,1}^j)\eta_{i,4}^j \\ \delta_{i,3}^j = \eta_{i,1}^j(1 - \eta_{i,4}^j) \\ \delta_{i,4}^j = \eta_{i,1}^j \eta_{i,4}^j \\ \delta_{i,5}^j = (1 - \eta_{i,1}^j)(1 - \eta_{i,4}^j) \end{cases} \tag{23}$$

Similarly, binary variables $\delta_{i,2}^j, \delta_{i,3}^j, \delta_{i,4}^j$ and $\delta_{i,5}^j$ can be modelled as Eq. 21 based on the Transformation Property 2 in Appendix A. Binary variables $\delta_{i,2}^j, \delta_{i,3}^j, \delta_{i,4}^j$ and $\delta_{i,5}^j$ correspond to Case 3, 4, 5 and 6 respectively. For example, when $\delta_{i,2}^j = 1, \min(t_i^j + A_i, t_{i+1}^{j-1} + A_{i+1}) = t_i^j + A_i$ and $\max(t_i^j, t_{i+1}^{j-1}) = t_i^j$, then $[\min(t_i^j + A_i, t_{i+1}^{j-1} + A_{i+1}) - \max(t_i^j, t_{i+1}^{j-1})] = t_i^j + A_i - t_i^j = A_i$, thus $\delta_{i,2}^j = 1$ means that the calculation of overlapping time is based on Case 3.

Based on the binary variables $\delta_{i,1}^j, \delta_{i,2}^j, \delta_{i,3}^j, \delta_{i,4}^j$ and $\delta_{i,5}^j$, the calculation of overlapping time Eq. 22 can be rewritten as:

$$\begin{cases} 0 \leqslant o_i^j \\ \widetilde{M}(\delta_{i,1}^j + \delta_{i,2}^j - 2) + A_i \leqslant o_i^j \\ \widetilde{M}(\delta_{i,1}^j + \delta_{i,3}^j - 2) + A_{i+1} \leqslant o_i^j \\ \widetilde{M}(\delta_{i,1}^j + \delta_{i,4}^j - 2) + (t_i^j + A_i - t_{i+1}^{j-1}) \leqslant o_i^j \\ \widetilde{M}(\delta_{i,1}^j + \delta_{i,5}^j - 2) + (t_{i+1}^{j-1} + A_{i+1} - t_i^j) \leqslant o_i^j \end{cases} \tag{24}$$

Considering minimizing the overlapping time, the value of o_i^j is depended on the value of the binary variables $\delta_{i,1}^j, \delta_{i,2}^j, \delta_{i,3}^j, \delta_{i,4}^j$ and $\delta_{i,5}^j$. For example, when $\delta_{i,1}^j = 0$, the second to fifth constraints of the above equation do not work, then $o_i^j = 0$; when $\delta_{i,1}^j = \delta_{i,2}^j = 1$, then $\delta_{i,3}^j = \delta_{i,4}^j = \delta_{i,5}^j = 0$, the second part of the above equation is the only effectual constraint, then $o_i^j = A_i$.

Besides, on the basis of the train traffic dynamics model, Eq. 24 can be rewritten with the vector and matrix form as:

$$F_1\delta_k + F_2 t_k + F_3 o_k + F_4 A \leqslant F_5 \tag{25}$$

where, $\delta_k = [\delta_1^{k-1}, \delta_2^{k-2}, \ldots, \delta_I^{k-I}]^T, \delta_i^j = [\delta_{i,1}^j, \delta_{i,2}^j, \delta_{i,3}^j, \delta_{i,4}^j, \delta_{i,5}^j]$;

$o_k = [o_1^{k-1}, o_2^{k-2}, \ldots, o_I^{k-I}]^T$; $A = [A_1, A_2, \ldots, A_I]^T$; the definitions of F_1, F_2, F_3, F_4 and F_5 are given in Appendix B. Meanwhile, the constraints of binary variables η_i^j and δ_i^j can also be rewritten with the vector and matrix form as:

$$E_1 t_k + E_2 \eta_k + E_3 A \leqslant E_4 \tag{26}$$

$$G_1\delta_k + G_2\eta_k \leqslant G_3 \tag{27}$$

where, $\eta_k = [\eta_1^{k-1}, \eta_2^{k-2}, \ldots, \eta_I^{k-I}]^T, \eta_i^j = [\eta_{i,1}^j, \eta_{i,2}^j, \eta_{i,3}^j, \eta_{i,4}^j]$; the definitions of $E_1, E_2, E_3, E_4, G_1, G_2$ and G_3 are given in Appendix B.

The above work finishes the computation of the overlapping time in the same direction. Similarly, the overlapping time in the opposite direction can be expressed in the same way. For the overlapping time in the opposite direction, the calculation is based on the relationship between $t_i^j, t_i^j + A_i, t_{2I-i+1}^{2I-j+1}$ and $t_{2I-i+1}^{2I-j+1} + A_{2I-i+1}$. Binary variables $\overline{\delta}_k = [\overline{\delta}_1^{k-1}, \overline{\delta}_2^{k-2}, \ldots, \overline{\delta}_I^{k-I}]^T$ and $\overline{\eta}_k = [\overline{\eta}_1^{k-1}, \overline{\eta}_2^{k-2}, \ldots, \overline{\eta}_I^{k-I}]^T$ are introduced to describe the overlapping time in the opposite direction $\overline{o}_k$:

$$\overline{F}_1\overline{\delta}_k + \overline{F}_2 t_k + \overline{F}_3\overline{o}_k + \overline{F}_4 A + \overline{F}_5\overline{t}_k + \overline{F}_6\overline{A} \leqslant \overline{F}_7 \tag{28}$$

and, related binary variables should meet the following constraints:

$$\overline{E}_1 t_k + \overline{E}_2\overline{\eta}_k + \overline{E}_3 A + \overline{E}_4\overline{t}_k + \overline{E}_5\overline{A} \leqslant \overline{E}_6 \tag{29}$$

$$\overline{G}_1\overline{\delta}_k + \overline{G}_2\overline{\eta}_k \leqslant \overline{G}_3 \tag{30}$$

where, $\overline{\delta}_i^j = [\overline{\delta}_{i,1}^j, \overline{\delta}_{i,2}^j, \overline{\delta}_{i,3}^j, \overline{\delta}_{i,4}^j, \overline{\delta}_{i,5}^j]^T$; $\overline{\eta}_i^j = [\overline{\eta}_{i,1}^j, \overline{\eta}_{i,2}^j, \overline{\eta}_{i,3}^j, \overline{\eta}_{i,4}^j]^T$;

$\overline{o}_k = [\overline{o}_1^{k-1}, \overline{o}_2^{k-2}, \ldots, \overline{o}_I^{k-I}]^T$; $\overline{t}_k = [t_{I+1}^{k-I-1}, t_{I+2}^{k-I-2}, \ldots, t_{2I}^{k-2I}]^T$, is the departure time in the down direction; $\overline{A} = [A_{I+1}, A_{I+2}, \ldots, A_{2I}]^T$, is the accelerating duration in the down direction; the derivation of Eq. 28–30 is given in Appendix B.

In addition, the calculation of overlapping time can be described as simpler forms:

$$\begin{cases} C_1 t_k + C_2 o_k + C_3\delta_k + C_4\eta_k \leqslant C_5 \\ \overline{C}_1 t_k + \overline{C}_2\overline{o}_k + \overline{C}_3\overline{\delta}_k + \overline{C}_4\overline{\eta}_k \leqslant \overline{C}_5 \end{cases} \tag{31}$$

where, the definitions of matrices in the above Eq. 31 are given in Appendix B.

2.3.3. Joint optimal control problem with minimizing overlapping time

The objectives of the joint optimal control problem are to minimize the timetable deviation, headway deviation, magnitude of the control actions (Zhang et al., 2019) and overlapping time between accelerating phases, which can be described as:

$$\begin{aligned} J_k = {} & p_1 x_{k+1}^T x_{k+1} + p_2(x_{k+1} - x_k)^T(x_{k+1} - x_k) + p_3 u r_k^T u r_k \\ & + p_3 u d_k^T u d_k + p_4 o_{k+1}^T o_{k+1} + \overline{p}_4 \overline{o}_{k+1}^T \overline{o}_{k+1} \end{aligned} \tag{32}$$

where, p_4 is the weight coefficient.

In addition, given the new objective function 32, by considering the traditional train regulation model 16, the joint optimal control problem with minimizing overlapping time can be formulated as the following joint optimal control problem:

$$\begin{cases} \min & \sum_{j_0}^{j_f}\{p_1 x_{k+1}^T x_{k+1} + p_2(x_{k+1}-x_k)^T(x_{k+1}-x_k) + p_3 u r_k^T u r_k \\ & \quad + p_3 u d_k^T u d_k + p_4 o_{k+1}^T o_{k+1} + \overline{p}_4 \overline{o}_{k+1}^T \overline{o}_{k+1}\} \\ \text{s.t.} & t_{k+1} = \Lambda t_k + T_{0,k} + R + u r_k + \omega r_k + D + u d_k + \omega d_k \\ & x_{k+1} = t_{k+1} - T_{k+1} \\ & C_1 t_{k+1} + C_2 o_{k+1} + C_3 \delta_{k+1} + C_4 \eta_{k+1} \leqslant C_5 \\ & \overline{C}_1 t_{k+1} + \overline{C}_2 \overline{o}_{k+1} + \overline{C}_3 \overline{\delta}_{k+1} + \overline{C}_4 \overline{\eta}_{k+1} \leqslant \overline{C}_5 \\ & \text{System constraints 15} \\ & \text{for } k \in \{j_0, \ldots, j_f\}. \end{cases} \tag{33}$$

2.4. Train regulation model with minimizing overlapping quantity

2.4.1. Overlapping quantity between accelerating phases

In this section, the overlapping quantity is proposed to replace the overlapping time as the indirect evaluation of substation peak power. The overlapping quantity indicates the number of valid overlapping. As shown in Fig. 4, when the accelerating peak power of train j is close to the accelerating peak power of train $2I-j-1$, there is a valid overlapping between these two trains. On the other hand, when the interval between two accelerating peak power is relatively large, the overlapping is invalid and the overlapping quantity will not increase. In this paper, the midpoint of the accelerating phase is regarded as the accelerating peak power point. For example, $t_i^j + A_i/2$ is the accelerating peak power point of train j running from station i to station $i+1$. As shown in Fig. 4, trains are accelerating simultaneously in the valid overlapping situation, which will cause substation peak power. Thus, the overlapping quantity is minimized to avoid the substation peak power in this section.

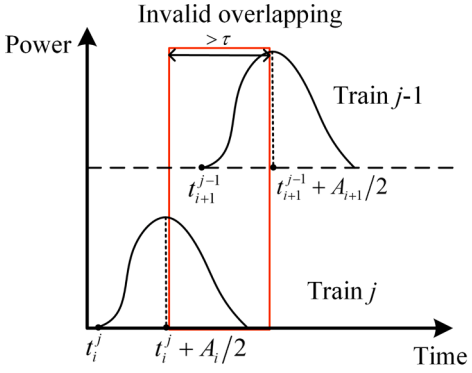

(a) adjacent trains in the same direction

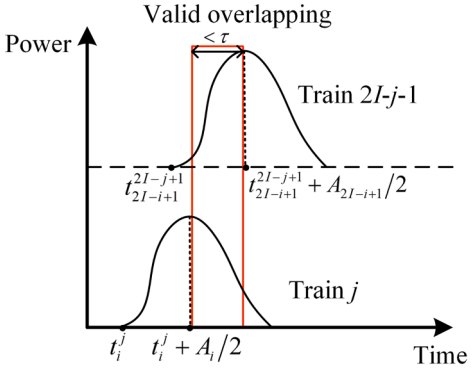

(b) adjacent trains in the opposite direction

Fig. 4. The illustration of the invalid and valid overlapping between accelerating phases.

Let τ be a measure of the validity of overlapping, when the interval between accelerating phases is larger than τ, the overlapping is invalid, otherwise, the overlapping is valid. The overlapping between train j leaving station i and train $j-1$ leaving station $i+1$ can be divided into two conditions as shown in Table 3.

2.4.2. Computation of overlapping quantity between accelerating phases

In order to distinguish these two conditions, as shown in Table 3, a binary variable α_i^j is introduced:

$$\alpha_i^j = 1 \Leftrightarrow \left| t_i^j + A_i/2 - t_{i+1}^{j-1} - A_{i+1}/2 \right| \leqslant \tau \tag{34}$$

where, $\left|t_i^j + A_i/2 - t_{i+1}^{j-1} - A_{i+1}/2\right| \leqslant \tau$ means that $t_i^j + A_i/2 - t_{i+1}^{j-1} - A_{i+1}/2 \leqslant \tau$ and $t_i^j + A_i/2 - t_{i+1}^{j-1} - A_{i+1}/2 \geqslant -\tau$. Then, two binary variables $\beta_{i,1}^j$ and $\beta_{i,2}^j$ are introduced:

$$\beta_{i,1}^j = 1 \Leftrightarrow t_i^j + A_i/2 - t_{i+1}^{j-1} - A_{i+1}/2 \leqslant \tau \tag{35}$$

$$\beta_{i,2}^j = 1 \Leftrightarrow t_i^j + A_i/2 - t_{i+1}^{j-1} - A_{i+1}/2 \geqslant -\tau \tag{36}$$

Based on the Transformation Property 2 in Appendix A, the implication of binary variables $\beta_{i,1}^j$ and $\beta_{i,2}^j$ can be modelled by the following linear constraints:

$$\begin{cases} t_i^j + A_i/2 - t_{i+1}^{j-1} - A_{i+1}/2 - \tau \leqslant \widetilde{M}(1-\beta_{i,1}^j) \\ t_i^j + A_i/2 - t_{i+1}^{j-1} - A_{i+1}/2 - \tau \geqslant -\widetilde{M}\beta_{i,1}^j \end{cases} \tag{37}$$

$$\begin{cases} -t_i^j - A_i/2 + t_{i+1}^{j-1} + A_{i+1}/2 - \tau \leqslant \widetilde{M}(1-\beta_{i,2}^j) \\ -t_i^j - A_i/2 + t_{i+1}^{j-1} + A_{i+1}/2 - \tau \geqslant -\widetilde{M}\beta_{i,2}^j \end{cases} \tag{38}$$

In addition, the binary variable α_i^j can be expressed as:

$$\alpha_i^j = \beta_{i,1}^j \beta_{i,2}^j \tag{39}$$

which means only when $\beta_{i,1}^j = 1$ and $\beta_{i,2}^j = 1, \alpha_i^j = 1$. The relationship between $\alpha_i^j, \beta_{i,1}^j$ and $\beta_{i,2}^j$ can be modelled by the following linear constrains:

$$\begin{cases} \alpha_i^j \leqslant \beta_{i,1}^j \\ \alpha_i^j \leqslant \beta_{i,2}^j \\ \alpha_i^j \geqslant \beta_{i,1}^j + \beta_{i,2}^j - 1 \end{cases} \tag{40}$$

When the interval between accelerating phases of train j leaving station i and train $j-1$ leaving station $i+1$ is less than $\tau, \alpha_i^j = 1$, which means there is valid overlapping. Then, the overlapping quantity can be expressed as $\sum \alpha_i^j$, which is minimized to suppress valid overlapping.

In addition, the calculation of overlapping quantity in the same and opposite direction can be described as the vector and matrix form as:

$$\begin{cases} B_1 t_k + B_2 \alpha_k + B_3 \beta_k \leqslant B_4 \\ \overline{B}_1 t_k + \overline{B}_2 \overline{\alpha}_k + \overline{B}_3 \overline{\beta}_k \leqslant \overline{B}_4 \end{cases} \tag{41}$$

where, $\alpha_k = [\alpha_1^{k-1}, \alpha_2^{k-2}, \ldots, \alpha_I^{k-I}]^T$; $\beta_k = [\beta_1^{k-1}; \beta_2^{k-2}; \ldots; \beta_I^{k-I}]$, $\beta_i^j =$

Table 3
Two conditions of the validity of overlapping.

Case	Condition	Overlapping	α_i^j
1	$\left\|t_i^j + A_i/2 - t_{i+1}^{j-1} - A_{i+1}/2\right\| \leqslant \tau$	Valid	1
2	$\left\|t_i^j + A_i/2 - t_{i+1}^{j-1} - A_{i+1}/2\right\| > \tau$	Invalid	0

$[\beta^j_{i,1}, \beta^j_{i,2}]^T$; $\overline{\alpha}_k = [\overline{\alpha}_1^{k-1}, \overline{\alpha}_2^{k-2}, \ldots, \overline{\alpha}_I^{k-I}]^T$; $\overline{\beta}_k = [\overline{\beta}_1^{k-1}; \overline{\beta}_2^{k-2}; \ldots; \overline{\beta}_I^{k-I}]$, $\overline{\beta}^j_i = [\overline{\beta}^j_{i,1}, \overline{\beta}^j_{i,2}]^T$; the definitions of other matrices in the above Eq. 41 are given in Appendix B.

2.4.3. Joint optimal control problem with minimizing overlapping quantity

The objectives of the joint optimal control problem is to minimize the timetable deviation, headway deviation, magnitude of the control actions (Zhang et al., 2019) and overlapping quantity, which can be described as:

$$\begin{aligned} J_k = {} & p_1 x_{k+1}^T x_{k+1} + p_2 (x_{k+1} - x_k)^T (x_{k+1} - x_k) + p_3 u r_k^T u r_k \\ & + p_3 u d_k^T u d_k + P_5 \alpha_{k+1} + \overline{P}_5 \overline{\alpha}_{k+1} \end{aligned} \tag{42}$$

where, $P_5 = [p_5, p_5, \ldots, p_5]_{1\times I}$; $\overline{P}_5 = [p_5, p_5, \ldots, p_5]_{1\times I}$; p_5 is the weight coefficient.

In addition, given the new objective function 42, by considering the traditional train regulation model 16, the joint optimal control problem with minimizing overlapping quantity can be formulated as the following joint optimal control problem:

$$\begin{cases} \min & \sum_{j_0}^{j_f} \{ p_1 x_{k+1}^T x_{k+1} + p_2 (x_{k+1} - x_k)^T (x_{k+1} - x_k) + p_3 u r_k^T u r_k \\ & \quad + p_3 u d_k^T u d_k + P_5 \alpha_{k+1} + \overline{P}_5 \overline{\alpha}_{k+1} \} \\ \text{s.t.} & t_{k+1} = \Lambda t_k + T_{0,k} + R + u r_k + \omega r_k + D + u d_k + \omega d_k \\ & x_{k+1} = t_{k+1} - T_{k+1} \\ & B_1 t_k + B_2 \alpha_k + B_3 \beta_k \leqslant B_4 \\ & \overline{B}_1 t_k + \overline{B}_2 \overline{\alpha}_k + \overline{B}_3 \overline{\beta}_k \leqslant \overline{B}_4 \\ & \text{System constraints 15} \\ & \text{for } k \in \{j_0, \ldots, j_f\}. \end{cases} \tag{43}$$

3. Algorithm description

3.1. Model predictive control algorithm

In this paper, MPC algorithm is adopted to solve the proposed optimal control problems (16), (33) and (43). First, since several parameters in the model, like ωr_k and ωd_k, are time-dynamics during the regulation process, the MPC algorithm as an online optimization technique can handle this character. Second, the MPC algorithm can effectively solve large-scale optimization problems, such as the proposed nonlinear high-dimensional problems.

MPC is a control algorithm that implements repeatedly optimal control in a rolling horizon manner. At each sample step k, an optimal control problem is solved based on the measured current system states at step k over a L step prediction horizon $(k+1, \ldots, k+L)$, and a set of optimal control sequence can be obtained. Then, only the first control action of the optimal control sequence is applied to the system considering the dynamics of the system parameters and disturbances. At the next step $k+1$, the optimal control problem is solved again based on the newly updated system states at step $k+1$, and also only the first control action is applied to the system, and repeat. Specifically, the MPC algorithm for the proposed problem can be described as the following three components.

Prediction model. The prediction model is used to predict the influence of control actions on the dynamic system. For the proposed train regulation problem, the train traffic dynamics model 5 is used to predict the timetable and headway deviations based on the system states at each step.

Optimization problem. At each step, a set of optimal control sequence is obtained by solving the optimization problem over a pre-given prediction horizon. Based on the joint optimal control model with minimizing overlapping time (33), at step k, the optimization problem with horizon L can be described as:

$$\begin{cases} \min & \sum_{i=0}^{L-1} \{ p_1 x_{k+i+1}^T x_{k+i+1} + p_2 [x_{k+i+1} - x_{k+i}]^T [x_{k+i+1} - x_{k+i}] \\ & + p_3 u r_{k+i}^T u r_{k+i} + p_3 u d_{k+i}^T u d_{k+i} + p_4 o_{k+i+1}^T o_{k+i+1} \\ & + \overline{p}_4 \overline{o}_{k+i+1}^T \overline{o}_{k+i+1} \} \\ \text{s.t.} & t_{k+i+1} = \Lambda t_{k+i} + T_{0,k+i} + R + u r_{k+i} + \omega r_{k+i} + D \\ & \qquad + u d_{k+i} + \omega d_{k+i} \\ & x_{k+i+1} = t_{k+i+1} - T_{k+i+1} \\ & \Psi_{min} \leqslant t_{k+i+1} - D - u d_{k+i} - \omega d_{k+i} - t_{k+i} \\ & D_{min} \leqslant D + u d_{k+i} + \omega d_{k+i} \\ & R_{min} \leqslant R + u r_{k+i} + \omega r_{k+i} \\ & UR_{min} \leqslant u r_{k+i} \leqslant UR_{max} \\ & UD_{min} \leqslant u d_{k+i} \leqslant UD_{max} \\ & C_1 t_{k+i+1} + C_2 o_{k+i+1} + C_3 \delta_{k+i+1} + C_4 \eta_{k+i+1} \leqslant C_5 \\ & \overline{C}_1 t_{k+i+1} + \overline{C}_2 \overline{o}_{k+i+1} + \overline{C}_3 \overline{\delta}_{k+i+1} + \overline{C}_4 \overline{\eta}_{k+i+1} \leqslant \overline{C}_5 \\ & \text{for } i \in \{0, \ldots, L-1\}. \end{cases} \tag{44}$$

The above optimization Problem 44 is a mixed integer quadratic programming (MIQP) problem, which can be solved by several effective solvers. Similarly, the joint optimal control problem with minimizing overlapping quantity (43) can be processed as a MIQP problem and the traditional optimal model (16) can be processed as a quadratic programming (QP) problem.

Rolling horizon. When the optimal control sequence is obtained by solving the optimization problem, the first control action is implemented to the system. At the next step, the input of the prediction model is the newly updated system states, the whole prediction horizon is shifted one step forward, and the optimization problem with newly updated parameters is solved again.

In addition, the MPC algorithm for the proposed train regulation problem can be summarized as follows. By applying the MPC algorithm, the optimal control problem is formulated as a set of MIQP/QP problems to obtain the control sequence. By choosing a proper prediction horizon length, the formulated MIQP problems can be solved effectively meeting the real-time computation requirement. Especially, in Step 2, the departure times of trains in the opposite direction are obtained to formulate the optimization problem.

Algorithm 1. MPC algorithm

Set $k = j_0$ and initialize the system states
repeat
Step 1: According to the system states and the prediction model, calculate the predicted states needed for the optimization problem in the prediction horizon from $k+1$ to $k+L$.
Step 2: Formulate the optimization problem.
Step 3: Solve the formulated optimization problem to obtain the optimal control sequence.
Step 4: Apply the first control action of the optimal control sequence, set $k = k+1$, and update the system states.
until $k \geqslant j_f$

3.2. The sizes of the optimization problems

The sizes of the optimization problems in MPC algorithm of traditional train regulation model (TR-T) (16), train regulation model with minimizing overlapping time (TR-OT) (33) and train regulation model with minimizing overlapping quantity (TR-OQ) (43) are shown in Table 4. In addition, the sizes of optimization problems are estimated for $I = 13$ (corresponding to 26 stations), and $L = 2$. As shown in Table 4,

Table 4
The sizes of the optimization problems.

Items	Size TR-T	TR-OT	TR-OQ	$I = 13$, $L = 2$ TR-T	TR-OT	TR-OQ
Constraints	$9IL$	$65IL$	$29IL$	234	1690	754
Continuous variables	$5IL$	$5IL$	$5IL$	130	130	130
Binary variables	0	$18IL$	$6IL$	0	468	156

the sizes of the optimization problems TR-OT and TR-OQ are larger than the size of the optimization problem TR-T. By comparing the optimization problems TR-OT and TR-OQ, we can observe that the size of the optimization problem TR-OQ is smaller, which means that using the overlapping quantity as the indirect evaluation of substation peak power can reduce the size of the train regulation problem considering the substation peak power reduction.

4. Numerical examples

4.1. Numerical example conditions

In order to illustrate the effectiveness robustness of the proposed models and algorithms, one of the Guangzhou metro lines is taken as an example to implement the numerical examples. This metro line includes 13 stations (i.e., $2I = 26$) and 7 substations, as shown in Fig. 5. Both the up and down direction operation of the metro line are considered in the numerical examples. Since disturbances occur frequently during peak hours, the morning peak hours is chosen as the train regulation testing period. During the morning peak hours, the nominal headway H is 150s, the minimum departure-arrival interval I_{min} is 20s, nominal timetable parameters are shown in Table 5. The constraints of the magnitude of the control actions are respectively set as $UR_{i,min} = -30$s, $UR_{i,max} = 30$s, $UD_{i,min} = -20$s, $UD_{i,mmax} = 20$s, $\forall i \in \{1, 2, \ldots, 2I\}$. In the numerical examples, 7:00 am is set as 0s, which is set as the initial stage ($k = 1$). The considered time step horizon ($j_f - j_s$) is 19, the departure time of the first train at station 1 in the up direction is 10s, and the departure time of the first train at station 14 in the down direction is 0s, then the departure times of trains at station 1 is $[10, 160, 310, \ldots, 2860]$s at station 17 is [0, 150, 300, …, 2850]s. At stage 1, there is no deviation between the nominal timetable and the actual timetable. Case studies are tested under the MATLAB environment on a personal computer with Intel Core i5 2.30 GHz CPU and 8 GB RAM, and the MIQP and QP problems are solved by using CPLEX Solver 12.6. Specially, the computation time at each stage is limited to be 60s.

To validate the effectiveness of the proposed real-time train regulation strategies considering minimizing the substation peak power (TR-OT and TR-OQ), they are compared with the traditional train regulation strategy (TR-T) and safe strategy without regulation (TR-S). More details about these four strategies are as follows:

Strategy TR-S. Safe strategy without regulation, the train regulation strategies are obtained only considering the system constraints (15). In the strategy TR-S, control actions are only adopted when the timetable is infeasible.

Table 5
Nominal timetable parameters during morning peak hours.

Station index	Nominal runtime [s]	Minimum runtime [s]	Accelerating duration [s]	Nominal dwelltime [s]	Minimum dwelltime [s]
1/26	0/125	0/110	27/0	60/60	45/45
2/25	129/82	110/68	22/28	45/45	30/30
3/24	86/115	75/102	25/24	45/45	30/30
4/23	116/80	103/68	20/22	45/45	30/30
5/22	81/108	71/94	24/20	45/45	30/30
6/21	111/110	98/100	24/20	50/50	30/30
7/20	102/120	91/102	27/28	44/44	30/30
8/19	124/99	115/82	22/25	46/46	30/30
9/18	99/75	93/66	20/25	47/45	30/30
10/17	74/80	65/70	20/20	55/55	45/45
11/16	75/90	66/85	23/25	50/50	30/30
12/15	96/129	85/110	28/20	48/45	30/30
13/14	131/0	120/0	0/28	60/60	45/45

Strategy TR-T. Traditional regulation strategy, the train regulation strategies are obtained by solving the traditional train regulation optimization problem (16) in the MPC algorithm. In the strategy TR-T, control actions are adopted to suppress disturbances by minimizing timetable deviation and headway deviation.

Strategy TR-OT. Regulation strategy considering minimizing the overlapping time, the train regulation strategies are obtained by solving the train regulation optimization problem considering minimizing the overlapping time (33) in the MPC algorithm. In the strategy TR-OT, the overlapping time is minimized to suppress the substation peak power.

Strategy TR-OQ. Regulation strategy considering minimizing the overlapping quantity, the train regulation strategies are obtained by solving the train regulation optimization problem considering minimizing the overlapping quantity (43) in the MPC algorithm. In the strategy TR-OQ, the overlapping quantity is minimized to suppress the substation peak power.

4.2. Comparison of different control strategies under pre-set disturbances

In this section, the runtime and dwelltime disturbances are pre-set artificially, which are shown in Table 6 and Table 7 respectively. Without loss of generality, the weight coefficients of timetable deviation, headway deviation and control actions are set to be the same (i.e. $p_1 = p_2 = p_3 = 1$). Meanwhile, in this section, the weight coefficient of overlapping time p_4 in the strategy TR-OT is set to be 1 (i.e. $p_4 = 1$), the weight coefficient of overlapping quantity p_5 in the strategy TR-OQ is set to be 1000 (i.e. $p_5 = 1000$). The prediction step horizon L is chosen as 2. The timetable deviations, headway deviations, timetables and train delays of four strategies are shown in Fig. 6, Fig. 7, Fig. 8 and Fig. 9 respectively. The performances of the four strategies are shown in Table 8. Specially, the total timetable deviation is defined as $[\sum_{i,j}(x_i^j)^2]^{\frac{1}{2}}$, and the total headway deviation is defined as $[\sum_{i,j}(x_i^j - x_i^{j-1})^2]^{\frac{1}{2}}$.

We compare the proposed strategies with other regulation strategies in the following aspects. The first aspect regards the timetable deviation.

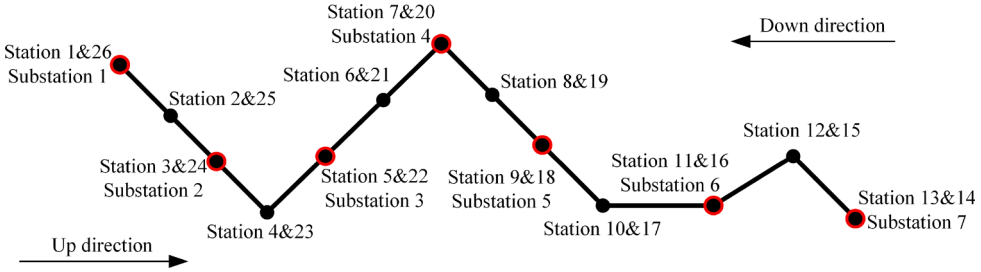

Fig. 5. The map of one of the Guangzhou metro line.

Table 6
The pre-set runtime disturbances *wr*.

Disturbance index	1	2	3	4	5	6	7	8	9	10	11	12
Stage index	1	1	3	3	11	11	15	15	4	6	12	15
Station index	3	8	3	12	4	10	2	8	16	22	24	15
Intensity [s]	30	30	25	25	30	25	30	20	20	20	30	30

Table 7
The pre-set dwelltime disturbances *wd*.

Disturbance index	1	2	3	4	5	6	7	8	9	10	11	12
Stage index	2	2	5	5	13	13	16	16	6	9	14	15
Station index	2	9	9	14	24	8	17	14	14	21	24	18
Intensity [s]	30	25	20	20	20	30	20	30	25	30	30	30

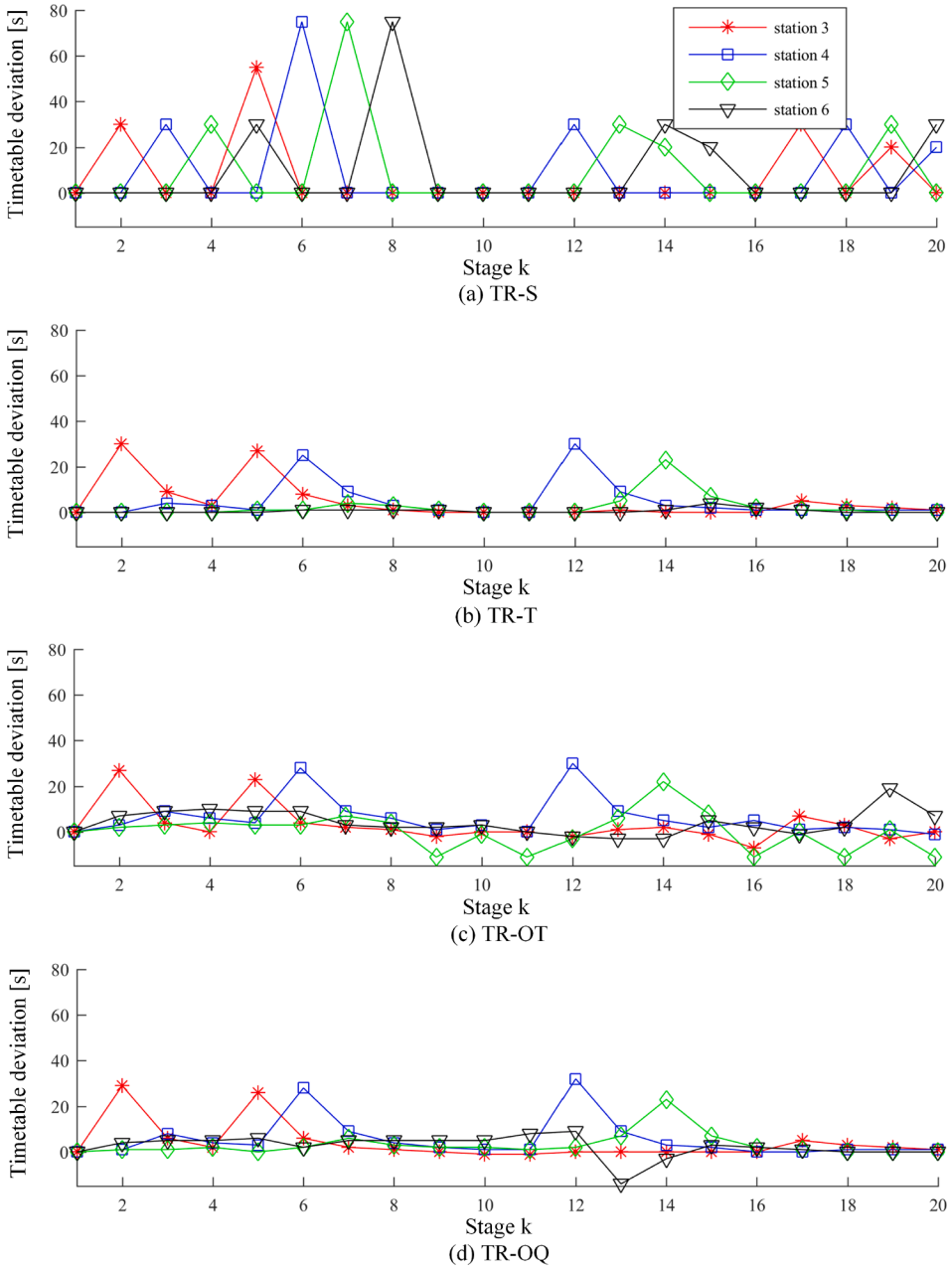

Fig. 6. The timetable deviations of four strategies under the pre-set disturbances.

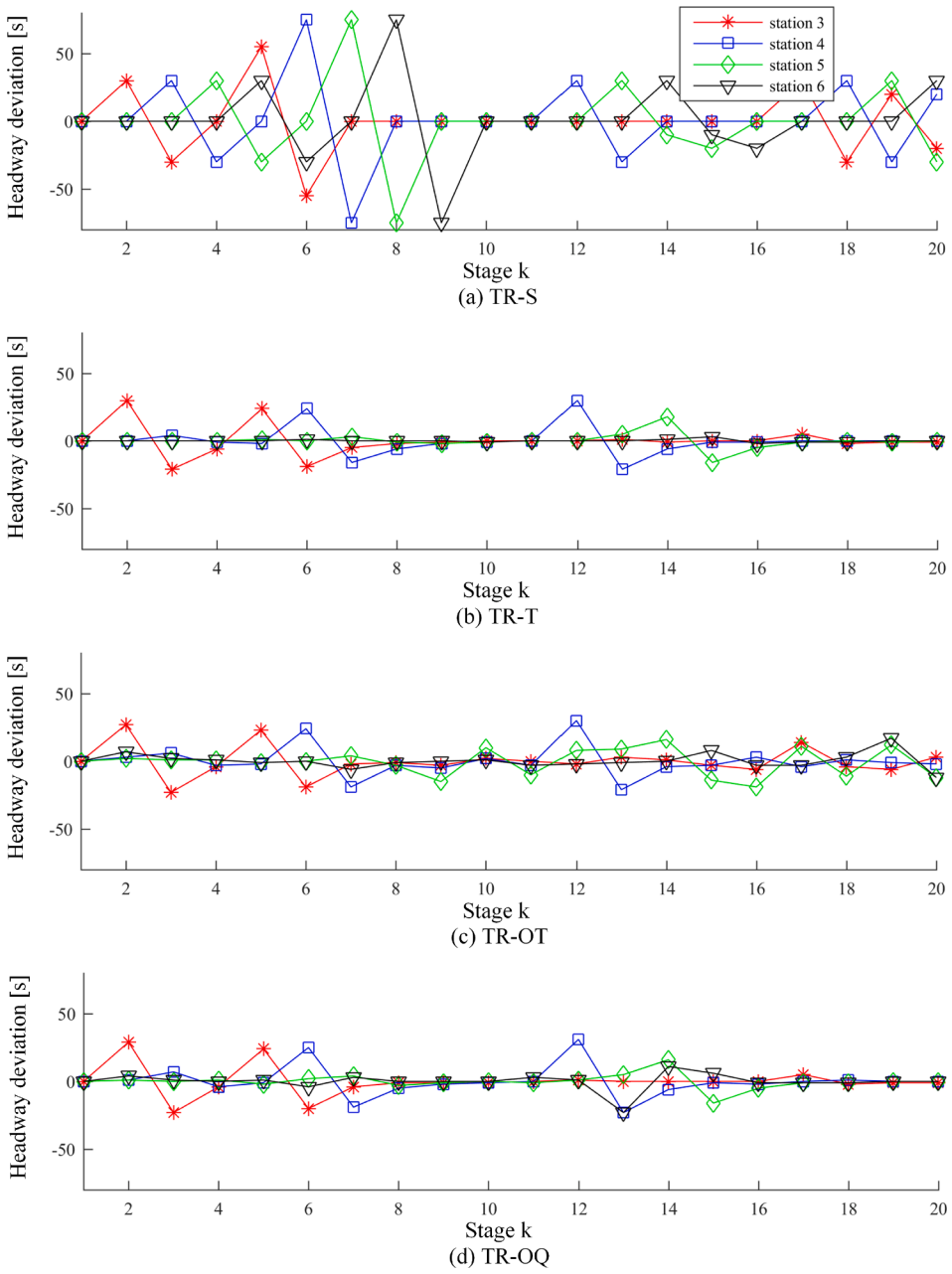

Fig. 7. The headway deviations of four strategies under the pre-set disturbances.

From Fig. 6, we can observe that the timetable deviations are significantly reduced in the strategies TR-T, TR-OT and TR-OQ, which indicates the stability of the URT line system under the optimal strategies. For the strategy TR-T, the timetable deviation at station 3 is reduced from 30s at stage 2 to 0s at stage 8, and trains are operated according to the nominal timetable as shown in Fig. 8 (b). For the strategies TR-OT and TR-OQ, the timetable deviations fluctuate in a small range and have no tendency to propagate as shown in Fig. 8 (c) and (d). However, the timetable deviations in the strategy TR-S are propagated to the latter stations without reduction, as shown in Fig. 8 (a), which will lead to instability of successive operation. In more details, as shown in Table 8, compared to the strategy TR-S, the total timetable deviations of the strategies TR-T, TR-OT and TR-OQ are reduced by 68.20%, 57.80% and 64.07% respectively. Meanwhile, the max timetable deviation is reduced from 100s to 34s, 39s and 40s respectively. Therefore, under the pre-set disturbances in this section, the strategy TR-T achieves the best performance in reducing the timetable deviation, and the strategy TR-OT and TR-OQ both achieve good performance in reducing the timetable deviation.

The second part is the headway deviation. From Fig. 7, we can observe that the headway deviations in the strategy fluctuate more frequently in a larger range in comparison to the strategies TR-T, TR-OT and TR-OQ. In more detail, as shown in Table 8, compared to the strategy TR-S, the total headway deviations of the strategy TR-T, TR-OT and TR-OQ are reduced by 73.84%, 66.86% and 71.84% respectively. Meanwhile, the max headway deviation is reduced from 100s to 31s, 32s and 37s respectively. Therefore, under the pre-set disturbances in this section, the strategy TR-T achieves the best performance in reducing the headway deviation, and the strategy TR-OT and TR-OQ both achieve good performance in reducing the headway deviation. The timetables for train 2 to 7 are shown in Fig. 8 and the delays for train 2 to 4 are shown in Fig. 9. For the strategy TR-S, the initial train delays are propagated to the latter stations and the train delays will increase when new disturbances occurring, as shown in Fig. 8 (a) and Fig. 9 (a). The

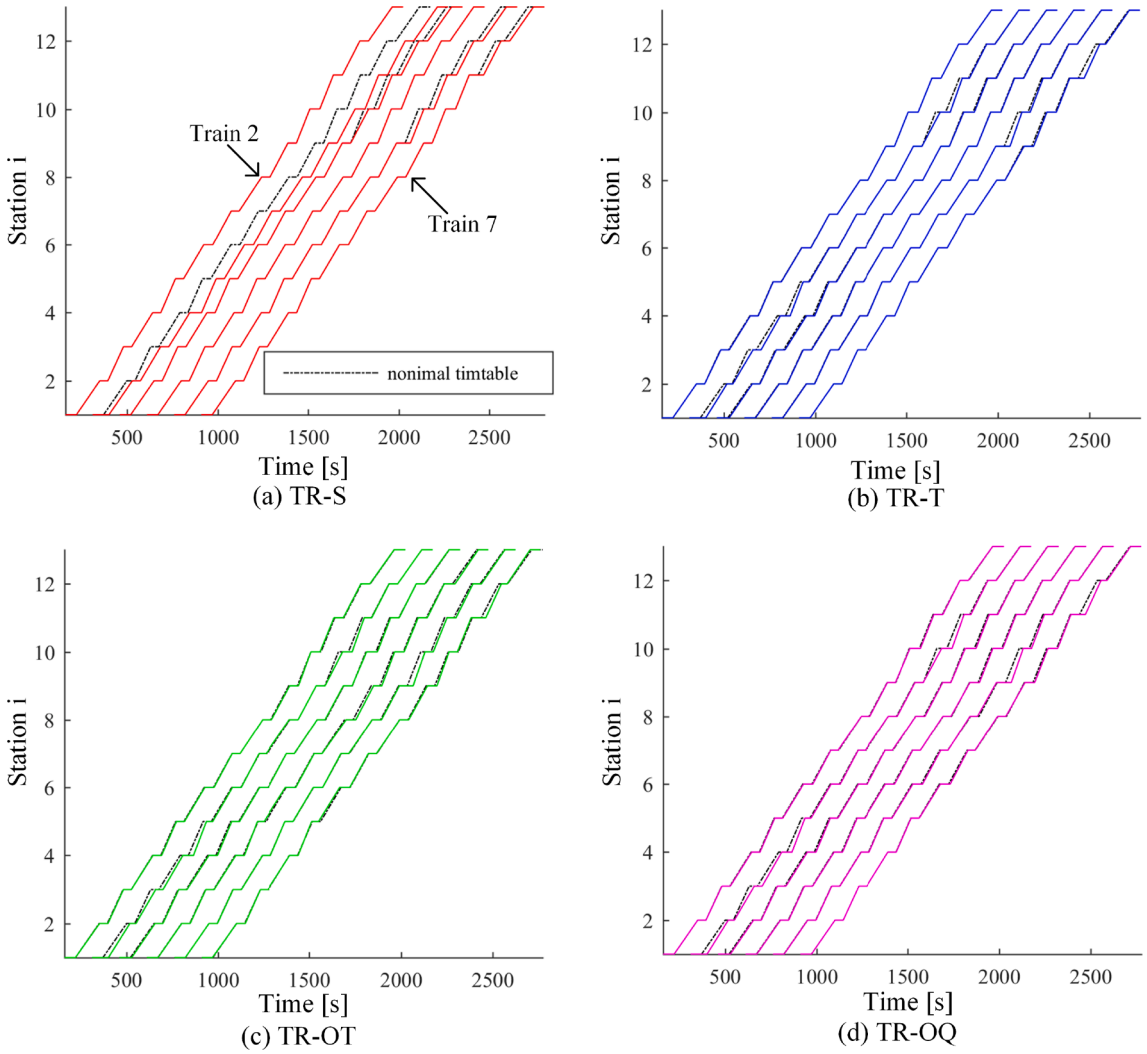

Fig. 8. The timetables for train 2 to 7 of four strategies under the pre-set disturbances.

incremental train delays will influence the nominal operation of successive and destroy the stability of the URT metro line system. On the other hand, the train delays are significantly reduced in the strategies TR-T, TR-OT and TR-OQ by applying the optimal train regulation strategies, as shown in Fig. 9 (b), (c) and (d) respectively, which indicates the stability of the URT line system under the optimal strategies.

The third point concerns the substation peak power. In this paper, the substation power over 4 MW is regarded as the peak power, it is due to that the maximum train traction power is around 4 MW. When the substation power exceeds 4 MW, it means there are multiple trains accelerating at the same time. As shown in Table 8, for the strategies TR-OT and TR-OQ, the total overlapping time is reduced from 195s to 174s and 168s compared to the strategy TR-T respectively, and the total overlapping quantity is reduced from 115 to 91 and 70 respectively. In addition, for the strategies TR-OT and TR-OQ, the duration of substation power over 4 MW is reduced from 753s to 745s and 701s compared to the strategy TR-T respectively. Under the pre-set disturbances in this section, by applying the strategies TR-OT and TR-OQ, the duration of substation peak power can be reduced in comparison to that of the strategy TR-T with the cost of weakening the effect of reducing the timetable and headway deviations.

The fourth aspect concerns real-time performance. As shown in Table 8, the average computation time of the strategies TR-T and TR-OQ are both less than 1s. The average computation time of the strategy TR-OT is 22.11s, which is less than the minimum dwelltime (i.e. 30s). However, in the strategy TR-OT, the computation time of solving the related optimal control problem is larger than 30s at some stages. Thus, besides the strategy TR-OT with the weight coefficient $p_4 = 1$, the above strategies can meet the real-time requirement.

4.3. Comparison of different control strategies under Monte-Carlo scheme

In this section, the train regulation strategies are evaluated in a Monte-Carlo scheme with respect to 30 different disturbance scenarios, aiming to better evaluate the effectiveness and robustness of the proposed train regulation methods. This number of scenarios, 30, is sufficient to obtain results with a level of confidence of 90% in train regulation problems (Ghasempour & Heydecker, 2020). Each scenario is formulated by sampling both runtime disturbances and dwelltime disturbances from Weibull distributions (Ghasempour & Heydecker, 2020; Quaglietta, Corman, & Goverde, 2013). We adopt shape parameter 1.5 and scale parameter 8s to produce runtime disturbances, as shown in Fig. 10 (a). Meanwhile, we adopt shape parameter 1.8 and scale parameter 4s to produce dwelltime disturbances. Especially, the scale parameter for dwelltime disturbances at interchange stations (Station 3 and 5) is set to be 6s, as shown in Fig. 10 (b). As shown in Fig. 10 (b), the probability of big dwelltime disturbances happening at interchange stations (the red line) is larger than it at other stations (the blue line). For this experiment, we adopt the same objective weight coefficients as in the previous section (i.e. $p_1 = p_2 = p_3 = p_4 = 1$ and $p_5 = 1000$), and the

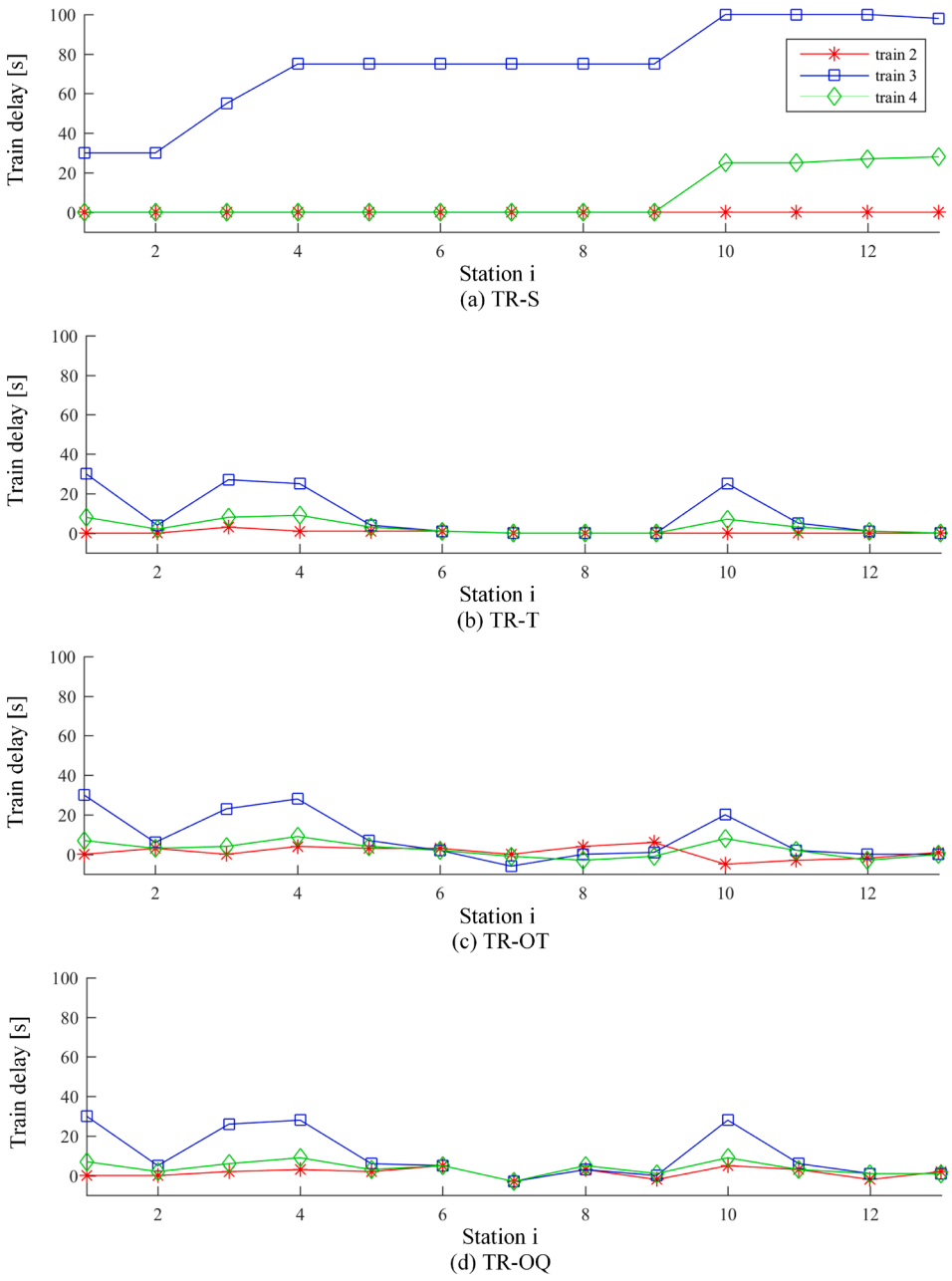

Fig. 9. The delays for train 2 to 4 of four strategies under the pre-set disturbances.

Table 8
The performances of four strategies under the pre-set disturbances.

Type of strategy	TR-S	TR-T	TR-OT	TR-OQ
Total timetable deviation [s]	372.15	118.36	157.06	133.70
Max timetable deviation [s]	100	34	39	40
Total headway deviation [s]	465.40	121.75	154.24	131.09
Max headway deviation [s]	100	31	32	37
Total overlapping time [s]	178	195	175	168
Total overlapping quantity	94	115	91	70
Duration of substation power over 4 MW [s]	708	753	745	701
Average computation time [s]	/	0.08	22.11	0.22

prediction step horizon L as 2. Since the train regulation strategies are evaluated in the Monte-Carlo scheme, the results are presented as average over the 30 disturbance scenarios considered. The performances (average of 30 scenarios) of four strategies are shown in Table 9.

From Table 9, we can observe that the timetable and headway deviations are significantly reduced in the strategies TR-T, TR-OT and TR-OQ, in comparison to the strategy TR-S. In terms of suppressing disturbances, the strategy TR-T achieves the best performances both in minimizing the timetable and headway deviations. In the strategy TR-T, the total timetable deviation is reduced to the minimum value, 330.89s, and the max timetable deviation is reduced to the minimum value, 41.21s. Meanwhile, the total headway deviation is reduced to the minimum value, 104.38s, and the max headway deviation is reduced to the

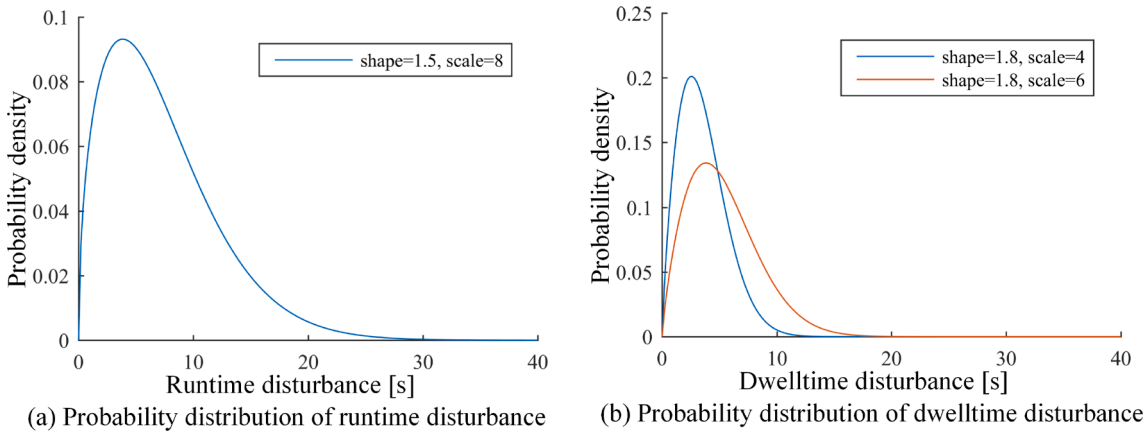

(a) Probability distribution of runtime disturbance (b) Probability distribution of dwelltime disturbance

Fig. 10. The probability distributions of runtime and dwelltime disturbances.

Table 9
The performances (average of 30 scenarios) of the four strategies under the Monte-Carlo scheme.

Type of strategy	TR-S	TR-T	TR-OT	TR-OQ
Total timetable deviation [s]	1132.26	330.89	347.26	341.02
Max timetable deviation [s]	165.43	41.21	44.26	42.81
Total headway deviation [s]	291.54	104.38	107.82	106.87
Max headway deviation [s]	58.50	22.57	23.21	23.21
Total overlapping time [s]	167.92	191.45	148.67	172.24
Total overlapping quantity	72.37	86.10	48.57	67.70
Duration of substation power over 4 MW [s]	629.43	1015.33	765.00	894.17
Average computation time [s]	/	0.05	8.69	0.18

minimum value, 22.57s. In terms of suppressing substation peak power, the strategies TR-OT and TR-OQ have better performances in reducing the duration of substation power over 4 MW in comparison to the strategy TR-T. By comparing the performances of the strategies TR-OT and TR-OQ, we can observe that the strategy TR-OT with weight coefficient $p_4 = 1$ have better performances in suppressing substation peak power in comparison to the strategy TR-OQ with coefficient $p_5 = 1000$, with the cost of weakening the effect of reducing the timetable and headway deviations. In terms of computation efficiency, the average computation times of the strategy TR-T and TR-OQ are both less than 1s, which meets the real-time requirements. Due to the complexity of the optimization problem solved at each stage, the average computation time of the strategy TR-OT reaches a large value, 8.69s.

In addition, we test cases where all disturbances are known in advance under the Monte-Carlo scheme, aiming to evaluate that how much is lost to the real-world disturbances. The performances of cases where all disturbances are known in advance are shown in Table 10. In comparison to cases where all disturbances are unknown in advance, as shown in Table 9, it is clear that the total timetable and headway deviations of cases that all disturbances are known in advance can be significantly reduced. For example, the total timetable deviation can be reduced from 330.89s to 38.64s by getting disturbance information in advance.

Table 10
The performances of cases where all disturbances are known in advance under the Monte-Carlo scheme.

Type of strategy	TR-T	TR-OT	TR-OQ
Total timetable deviation [s]	38.64	80.22	70.81
Max timetable deviation [s]	6.36	12.25	9.68
Total headway deviation [s]	17.22	13.95	15.19
Max headway deviation [s]	3.45	2.82	4.07
Total overlapping time [s]	197.39	109.63	145.80
Total overlapping quantity	124.23	25.40	84.27
Duration of substation power over 4 MW [s]	723.83	628.73	696.73
Average computation time [s]	0.40	11.85	0.22

4.4. Comparison of different prediction horizon length L

In this section, we analyze the impact of the prediction horizon length L on the computational complexity and regulation performances. The strategies TR-T, TR-OT and TR-OQ with different prediction horizon lengths are evaluated under the Monte-Carlo scheme with respect to 30 different disturbance scenarios. The results of the strategies TR-T, TR-OT and TR-OQ are shown in Tables 11–13 respectively. It is clear that with the increase of prediction horizon length L from 1 to 5, the average computation times of the strategies TR-T, TR-OT and TR-OQ increase. Although the computation time quickly increases from $L = 2$ to $L = 3$, higher values for L do not seem to negatively impact solving times of the strategy TR-OT as much. It is due to the pre-set computation time limit at each stage. Meanwhile, the sizes of the optimization problems, as shown in Table 4, reflect that the prediction horizon length L has a significant impact on the computation complexity. On the other hand, the regulation performances are influenced by the prediction horizon length L. When L increases from 1 to 2, the performances are improved significantly in all strategies, as shown in Table 11, Table 12 and Table 13, like the total timetable deviation of the strategy TR-OT is reduced from 418.29s to 347.26s. However, when L increases from 2 to 5, the

Table 11
The performances of TR-T strategy with different prediction horizon length L.

Value of L	1	2	3	4	5
Total timetable deviation [s]	407.36	330.89	318.35	315.96	315.49
Max timetable deviation [s]	47.21	41.21	40.25	40.07	40.04
Total headway deviation [s]	103.31	104.38	104.48	104.48	104.48
Max headway deviation [s]	22.84	22.57	22.54	22.53	22.53
Total overlapping time [s]	199.05	191.45	190.54	190.39	190.36
Total overlapping quantity	93.2	86.10	85.6	85.57	85.53
Duration of substation power over 4 MW [s]	1032.83	1015.33	1013.13	1014.90	1015.17
Average computation time [s]	0.02	0.05	0.13	0.22	0.51

Table 12
The performances of TR-OT strategy with different prediction horizon length L.

Value of L	1	2	3	4	5
Total timetable deviation [s]	418.29	347.26	337.03	335.26	334.93
Max timetable deviation [s]	50.18	44.26	43.42	43.28	43.25
Total headway deviation [s]	107.58	107.82	107.85	107.84	107.84
Max headway deviation [s]	23.74	23.21	23.17	23.17	23.16
Total overlapping time [s]	148.25	148.67	148.31	148.15	148.11
Total overlapping quantity	47.73	48.57	47.87	47.70	47.70
Duration of substation power over 4 MW [s]	757.97	765.00	767.83	768.03	767.60
Average computation time [s]	0.38	8.69	318.53	408.32	432.79

Table 13
The performances of TR-OQ strategy with different prediction horizon length L.

Value of L	1	2	3	4	5
Total timetable deviation [s]	413.89	341.02	330.35	328.88	328.70
Max timetable deviation [s]	48.97	42.81	42.00	41.91	41.90
Total headway deviation [s]	106.76	106.87	109.31	109.28	109.23
Max headway deviation [s]	23.89	23.21	25.40	25.36	25.36
Total overlapping time [s]	179.68	172.24	171.54	171.50	171.51
Total overlapping quantity	73.20	67.70	68.13	68.07	68.10
Duration of substation power over 4 MW [s]	891.13	894.17	895.83	895.57	895.00
Average computation time [s]	0.06	0.18	0.41	0.65	0.97

performances are not improved with the cost of computation time increase. Therefore, considering the computational complexity and regulation performances, it is reasonable to set the prediction horizon length L as 2.

4.5. Comparison of different objective weight coefficients

To balance the objectives better, we aim to conduct the sensitivity analysis for the weight coefficients p_4 and p_5. The weight coefficient p_4 is related to the overlapping time, and p_5 is related to the overlapping quantity. By only changing weight coefficients p_4 or p_5, its effects on the regulation performances are evaluated. In this section, two groups of numerical experiments are set up under the Monte-Carlo scheme. In the first group, the weight coefficient p_4 is changed with the values of 0, 1, 10, 100 and 1000, to analyze the effect of the overlapping time on the regulation performances. And, in the second group, the weight coefficient p_5 is changed with the values of 0, 100, 500, 1000, and 20000, to analyze the effect of the overlapping quantity on the regulation performances.

Table 14
The performances of TR-OT strategy with different objective weight coefficient p_4.

Value of p_4	0	1	10	100	1000
Total timetable deviation [s]	330.89	347.26	434.50	508.26	572.18
Max timetable deviation [s]	41.21	44.26	59.80	85.43	94.45
Total headway deviation [s]	104.38	107.82	135.63	251.14	323.63
Max headway deviation [s]	22.57	23.21	34.61	66.19	80.44
Total overlapping time [s]	191.45	148.67	112.65	92.61	85.71
Total overlapping quantity	86.10	48.57	27.07	19.17	16.63
Duration of substation power over 4 MW [s]	1015.33	765.00	528.60	478.80	468.43
Average computation time [s]	0.05	8.69	28.62	78.77	94.44

Table 15
The performances of TR-OQ strategy with different objective weight coefficient p_5.

Value of p_5	0	100	500	1000	2000
Total timetable deviation [s]	330.89	339.09	341.02	341.02	341.03
Max timetable deviation [s]	41.21	42.44	42.81	42.81	42.81
Total headway deviation [s]	104.38	106.43	106.87	106.87	106.87
Max headway deviation [s]	22.57	22.83	23.21	23.21	23.21
Total overlapping time [s]	191.45	174.13	172.24	172.24	172.24
Total overlapping quantity	86.10	69.77	67.70	67.70	67.70
Duration of substation power over 4 MW [s]	1015.33	900.23	894.17	894.17	894.17
Average computation time [s]	0.05	0.24	0.18	0.18	0.16

As shown in Table 14, the weight coefficient p_4 has a significant influence on the duration of substation power over 4 MW. The duration of substation power over 4 MW decreases as the value of p_4 increases. The duration is 765.00s with $p_4 = 1$, and the duration is reduced to 468.43s when $p_4 = 1000$. However, at the same time, the total timetable deviation increases from 347.26s to 572.18s, and the total headway deviation increases from 107.82s to 323.63s. Therefore, it is necessary to balance the objective of reducing the substation peak power and the objectives of reducing the timetable and headway deviations by picking a suitable value of p_4. Meanwhile, the weight coefficient p_5 has the same influence on the objectives. As shown in Table 15, when the value of p_5 increases, the duration of substation power over 4 MW decreases, and the timetable and headway deviations increase. Specially, when p_5 increases from 500 to 2000, there is no significant change in the performances, like the duration of substation power over 4 MW maintains at 894.17s. It is the limitation of substation peak power reduction that can be achieved through the strategy TR-OQ. By comparing the strategies TR-OT and TR-OQ with different objective weights, it is clear that the strategy TR-OT has more potential for suppressing substation peak power.

5. Conclusions

In this paper, we studied the real-time train regulation optimization problem under disturbances to suppress the train delays and substation peak power. We introduced two novel indirect indicators (i.e. overlapping time between accelerating phases, overlapping quantity between accelerating phases), which were minimized to reduce substation peak power in the train regulation problem. In addition, based on the train traffic dynamics model, we developed joint optimal train regulation models for minimizing the timetable deviation, headway deviation and substation peak power. To capture the model complexity and real-time requirements for the train regulation problem, real-time control algorithms based on MPC were designed, in which the optimal train regulation strategies were generated at each control cycle.

Numerical examples based on one of the Guangzhou metro lines were implemented to demonstrate the performance of the proposed approaches. The computational results showed that train regulation strategies considering substation peak power reduction can effectively minimize the duration of peak power and the timetable and headway deviations. Moreover, the computation time of generating the optimal solution with minimizing the overlapping quantity by the MPC algorithm was only around 0.2s, which satisfied the real-time requirement.

Our future research will focus on the train regulation problem under large perturbations (disruptions). This paper only deals with the train regulation problem under small perturbations (disturbances). On the

other hand, train connections at terminal stations will be considered in the train regulation method so as to provide a feasible scheme.

CRediT authorship contribution statement

Bo Jin: Writing - original draft, Writing - review & editing, Methodology, Software. **Xiaoyun Feng:** Conceptualization, Supervision. **Qingyuan Wang:** Visualization, Supervision. **Pengfei Sun:** Visualization, Formal analysis, Conceptualization.

Acknowledgements

This work was supported by the National Natural Science Foundation of China (Nos. U1934221, 62003283).

Appendix A. Transformation properties

Based on the study (Bemporad & Morari, 1999), two transformation properties are introduced.

Transformation Property 1. Consider the statement $\widetilde{f}(\widetilde{x})\leqslant 0$, where $\widetilde{f}: R^n \to R$ is affince, $\widetilde{x} \in \chi$ with $\chi \subset R^n$.

The condition $\widetilde{f}(\widetilde{x})\leqslant 0$ can be expressed by a logical variable $\delta \in \{0,1\}, \widetilde{f}(\widetilde{x})\leqslant 0 \Leftrightarrow \delta = 1$ is equivalent to

$$\begin{cases} \widetilde{f}(\widetilde{x}) \leqslant \widetilde{M}(1-\delta) \\ \widetilde{f}(\widetilde{x}) \geqslant \varepsilon + (\widetilde{m}-\varepsilon)\delta \end{cases} \tag{45}$$

where, $\widetilde{M} = \max \widetilde{f}(\widetilde{x})$ and $\widetilde{m} = \min \widetilde{f}(\widetilde{x})$.

Transformation Property 2. The product of two logical variables $\delta_1\delta_2$ can be replaced by an auxiliary logical variable $\delta_3 = \delta_1\delta_2$, i.e. $[\delta_3 = 1] \Leftrightarrow [\delta_1 = 1]$ and $[\delta_2 = 1]$, which is equivalent to

$$\begin{cases} -\delta_1 + \delta_3 \leqslant 0 \\ -\delta_2 + \delta_3 \leqslant 0 \\ \delta_1 + \delta_2 - \delta_3 \leqslant 1 \end{cases} \tag{46}$$

Appendix B. Definition of matrices

The definitions of matrices in Eqs. (25)–(31) are as follows:

$$f_1 = \begin{bmatrix} 0 & 0 & 0 & 0 & 0 \\ \widetilde{M} & \widetilde{M} & 0 & 0 & 0 \\ \widetilde{M} & 0 & \widetilde{M} & 0 & 0 \\ \widetilde{M} & 0 & 0 & \widetilde{M} & 0 \\ \widetilde{M} & 0 & 0 & 0 & \widetilde{M} \end{bmatrix};$$

$$f_2 = [0,0,0,1,-1]^T; f_3 = [0,0,0,-1,1]^T; f_4 = [-1,-1,-1,-1,-1]^T;$$

$$f_5 = [0,1,0,1,0]^T; f_6 = [0,0,1,0,1]^T; f_7 = [0, 2\widetilde{M}, 2\widetilde{M}, 2\widetilde{M}, 2\widetilde{M}]^T.$$

$$F_1 = \mathrm{diag}\{f_1\}_{5I\times 5I}; F_3 = \mathrm{diag}\{f_4\}_{5I\times I}; F_5 = [f_7; f_7; \ldots; f_7]_{5I\times 1};$$

$$F_2 = \begin{bmatrix} f_2 & f_3 & 0 & 0 & \ldots \\ 0 & f_2 & f_3 & 0 & \ldots \\ \ldots & \ldots & \ldots & \ldots & \ldots \\ 0 & \ldots & \ldots & f_2 & f_3 \\ 0 & \ldots & \ldots & \ldots & f_2 \end{bmatrix}_{5I\times I}; F_4 = \begin{bmatrix} f_5 & f_6 & 0 & 0 & \ldots \\ 0 & f_5 & f_6 & 0 & \ldots \\ \ldots & \ldots & \ldots & \ldots & \ldots \\ 0 & \ldots & \ldots & f_5 & f_6 \\ 0 & \ldots & \ldots & \ldots & f_5 \end{bmatrix}_{5I\times I};$$

$$e_1 = [1,-1,1,-1,1,-1,1,-1]^T; e_2 = [-1,1,-1,1,-1,1,-1,1]^T;$$

$$e_3 = \begin{bmatrix} \widetilde{M} & \varepsilon-\widetilde{m} & 0 & 0 & 0 & 0 & 0 & 0 \\ 0 & 0 & \widetilde{M} & \varepsilon-\widetilde{m} & 0 & 0 & 0 & 0 \\ 0 & 0 & 0 & 0 & \widetilde{M} & \varepsilon-\widetilde{m} & 0 & 0 \\ 0 & 0 & 0 & 0 & 0 & 0 & \widetilde{M} & \varepsilon-\widetilde{m} \end{bmatrix}^T;$$

$$e_4 = [0,0,0,0,1,-1,1,-1]^T; e_5 = [0,0,-1,1,0,0,-1,1]^T;$$

$$e_6 = [\widetilde{M}, -\varepsilon, \widetilde{M}, -\varepsilon, \widetilde{M}, -\varepsilon, \widetilde{M}, -\varepsilon]^T;$$

$$E_1 = \begin{bmatrix} e_1 & e_2 & 0 & 0 & \ldots \\ 0 & e_1 & e_2 & 0 & \ldots \\ \ldots & \ldots & \ldots & \ldots & \ldots \\ 0 & \ldots & \ldots & e_1 & e_2 \\ 0 & \ldots & \ldots & \ldots & e_1 \end{bmatrix}_{8I\times I}; E_3 = \begin{bmatrix} e_4 & e_5 & 0 & 0 & \ldots \\ 0 & e_4 & e_5 & 0 & \ldots \\ \ldots & \ldots & \ldots & \ldots & \ldots \\ 0 & \ldots & \ldots & e_4 & e_5 \\ 0 & \ldots & \ldots & \ldots & e_4 \end{bmatrix}_{8I\times I};$$

$$E_2 = \mathrm{diag}\{e_3\}_{8I\times 4I}; E_4 = [e_6; e_6; \ldots; e_6]_{8I\times 1};$$

$$g_1 = \begin{bmatrix} -1 & 1 & 1 & 0 & 0 & 0 & 0 & 0 & 0 & 0 & 0 & 0 & 0 & 0 & 0 \\ 0 & 0 & 0 & -1 & 1 & 1 & 0 & 0 & 0 & 0 & 0 & 0 & 0 & 0 & 0 \\ 0 & 0 & 0 & 0 & 0 & 0 & -1 & 1 & 1 & 0 & 0 & 0 & 0 & 0 & 0 \\ 0 & 0 & 0 & 0 & 0 & 0 & 0 & 0 & 0 & -1 & 1 & 1 & 0 & 0 & 0 \\ 0 & 0 & 0 & 0 & 0 & 0 & 0 & 0 & 0 & 0 & 0 & 0 & -1 & 1 & 1 \end{bmatrix}^T;$$

$$g_2 = \begin{bmatrix} 0 & 0 & 0 & -1 & 0 & 1 & 1 & -1 & 0 & 1 & -1 & 0 & -1 & 1 & 0 \\ 1 & -1 & 0 & 0 & 0 & 0 & 0 & 0 & 0 & 0 & 0 & 0 & 0 & 0 & 0 \\ -1 & 0 & -1 & 0 & 0 & 0 & 0 & 0 & 0 & 0 & 0 & 0 & 0 & 0 & 0 \\ 0 & 0 & 0 & 1 & -1 & 0 & -1 & 0 & 1 & 1 & 0 & -1 & -1 & 0 & 1 \end{bmatrix}^T;$$

$g_3 = [0,0,1,0,0,1,0,0,1,1,0,0,-1,1,1]^T$;
$G_1 = \mathrm{diag}\{g_1\}_{15I\times 5I}$; $G_2 = \mathrm{diag}\{g_2\}_{15I\times 4I}$; $G_3 = [g_3; g_3; \ldots; g_3]_{15I\times 1}$.

$$C_1 = \begin{bmatrix} F_2 \\ E_1 \\ 0 \\ \vdots \\ 0 \end{bmatrix}_{28I\times I}; C_2 = \begin{bmatrix} F_3 \\ 0 \\ \vdots \\ 0 \end{bmatrix}_{28I\times I}; C_3 = \begin{bmatrix} F_1 \\ 0 \\ \vdots \\ 0 \\ G_1 \end{bmatrix}_{28I\times 5I};$$

$$C_4 = \begin{bmatrix} 0 \\ \vdots \\ 0 \\ E_2 \\ G_2 \end{bmatrix}_{28I\times 4I}; C_5 = \begin{bmatrix} F_5 - F_4A \\ E_4 - E_3A \\ G_3 \end{bmatrix}_{28I\times 1};$$

The definitions of $\overline{\eta}_{i,1}^j, \overline{\eta}_{i,2}^j, \overline{\eta}_{i,3}^j$ and $\overline{\eta}_{i,4}^j$ are as follows:

$$\begin{cases} \overline{\eta}_{i,1}^j = 1 \Leftrightarrow t_i^j \leqslant t_{2I-i+1}^{2I-j+1} \\ \overline{\eta}_{i,2}^j = 1 \Leftrightarrow t_i^j \leqslant t_{2I-i+1}^{2I-j+1} + A_{2I-i+1} \\ \overline{\eta}_{i,3}^j = 1 \Leftrightarrow t_i^j + A_i \leqslant t_{2I-i+1}^{2I-j+1} \\ \overline{\eta}_{i,4}^j = 1 \Leftrightarrow t_i^j + A_i \leqslant t_{2I-i+1}^{2I-j+1} + A_{2I-i+1} \end{cases};$$

The definitions of $\overline{\delta}_{i,1}^j, \overline{\delta}_{i,2}^j, \overline{\delta}_{i,3}^j, \overline{\delta}_{i,4}^j$ and $\overline{\delta}_{i,5}^j$ are as follows:

$$\begin{cases} \overline{\delta}_{i,1}^j = \overline{\eta}_{i,2}^j(1 - \overline{\eta}_{i,3}^j) \\ \overline{\delta}_{i,2}^j = (1 - \overline{\eta}_{i,1}^j)\overline{\eta}_{i,4}^j \\ \overline{\delta}_{i,3}^j = \overline{\eta}_{i,1}^j(1 - \overline{\eta}_{i,4}^j) \\ \overline{\delta}_{i,4}^j = \overline{\eta}_{i,1}^j\overline{\eta}_{i,4}^j \\ \overline{\delta}_{i,5}^j = (1 - \overline{\eta}_{i,1}^j)(1 - \overline{\eta}_{i,4}^j) \end{cases};$$

$\overline{F}_1 = \mathrm{diag}(f_1)_{5I\times 5I}$; $\overline{F}_2 = \mathrm{diag}(f_2)_{5I\times I}$; $\overline{F}_3 = \mathrm{diag}(f_4)_{5I\times I}$;
$\overline{F}_4 = \mathrm{diag}(f_5)_{5I\times I}$; $\overline{F}_7 = \mathrm{diag}(f_7)_{5I\times 1}$;

$$\overline{F}_5 = \begin{bmatrix} 0 & \ldots & 0 & f_3 \\ 0 & \ldots & f_3 & 0 \\ \ldots & \ldots & \ldots & \ldots \\ f_3 & \ldots & 0 & 0 \end{bmatrix}_{5I\times I}; \overline{F}_6 = \begin{bmatrix} 0 & \ldots & 0 & f_6 \\ 0 & \ldots & f_6 & 0 \\ \ldots & \ldots & \ldots & \ldots \\ f_6 & \ldots & 0 & 0 \end{bmatrix}_{5I\times I};$$

$\overline{E_1} = \mathrm{diag}(e_1)_{8I\times I}$; $\overline{E_2} = \mathrm{diag}(e_3)_{8I\times 4I}$; $\overline{E_3} = \mathrm{diag}(e_4)_{8I\times 4I}$;

$$\overline{E_4} = \begin{bmatrix} 0 & \ldots & 0 & e_2 \\ 0 & \ldots & e_2 & 0 \\ \ldots & \ldots & \ldots & \ldots \\ e_2 & \ldots & 0 & 0 \end{bmatrix}_{8I\times I}; \overline{E_5} = \begin{bmatrix} 0 & \ldots & 0 & e_5 \\ 0 & \ldots & e_5 & 0 \\ \ldots & \ldots & \ldots & \ldots \\ e_5 & \ldots & 0 & 0 \end{bmatrix}_{8I\times 2I};$$

$\overline{E_6} = [e_6; e_6; \ldots; e_6]_{8I\times 1}$;
$\overline{G}_1 = \mathrm{diag}(g_1)_{15I\times 5I}$; $\overline{G}_2 = \mathrm{diag}(g_2)_{15I\times 4I}$; $\overline{G}_3 = \mathrm{diag}(g_3)_{15I\times 1}$.

$$\overline{C}_1 = \begin{bmatrix} \overline{F}_2 \\ \overline{E}_1 \\ 0 \\ \vdots \\ 0 \end{bmatrix}_{28I\times I}; \overline{C}_2 = \begin{bmatrix} \overline{F}_3 \\ 0 \\ \vdots \\ 0 \end{bmatrix}_{28I\times I}; \overline{C}_3 = \begin{bmatrix} \overline{F}_1 \\ 0 \\ \vdots \\ 0 \\ \overline{G}_1 \end{bmatrix}_{28I\times 5I};$$

$$\overline{C}_4 = \begin{bmatrix} 0 \\ \vdots \\ 0 \\ \overline{E}_2 \\ \overline{G}_2 \end{bmatrix}_{28I\times 4I}; \overline{C}_5 = \begin{bmatrix} \overline{F}_7 - \overline{F}_5\bar{t}_k - \overline{F}_6\overline{A} \\ \overline{E}_4 - \overline{E}_4\bar{t}_k - \overline{E}_5\overline{A} \\ \overline{G}_3 \end{bmatrix}_{28I\times 1};$$

The definitions of matrices in Eq. 41 are as follows:

$q_1 = [1,-1,-1,1]^T$; $q_2 = [-1,1,1,-1]^T$; $q_3 = [\widetilde{M}, -\widetilde{M}, \widetilde{M}, -\widetilde{M}]^T$;
$q_4 = [1/2,-1/2,-1/2,1/2]^T$; $q_5 = [-1/2,1/2,1/2,-1/2]^T$;
$q_6 = [\widetilde{M}+\tau, -\tau, \widetilde{M}+\tau, -\tau]^T$; $s_1 = [1,1,-1]^T$; $s_2 = [-1,0;0,-1;1,1]$;
$s_3 = [0,0,1]^T$;

$$Q_1 = \begin{bmatrix} q_1 & q_2 & 0 & 0 & \ldots \\ 0 & q_1 & q_2 & 0 & \ldots \\ \ldots & \ldots & \ldots & \ldots & \ldots \\ 0 & \ldots & \ldots & q_1 & q_2 \\ 0 & \ldots & \ldots & \ldots & q_1 \end{bmatrix}_{4I\times I}; Q_3 = \begin{bmatrix} q_4 & q_5 & 0 & 0 & \ldots \\ 0 & q_4 & q_5 & 0 & \ldots \\ \ldots & \ldots & \ldots & \ldots & \ldots \\ 0 & \ldots & \ldots & q_4 & q_5 \\ 0 & \ldots & \ldots & \ldots & q_4 \end{bmatrix}_{4I\times I};$$

$Q_2 = \mathrm{diag}(q_4)_{4I\times 2I}$; $Q_4 = [q_6; q_6; \ldots; q_6]_{4I\times 1}$;
$S_1 = \mathrm{diag}(s_1)_{3I\times I}$; $S_2 = \mathrm{diag}(s_2)_{3I\times 2I}$; $S_3 = [s_3; s_3; \ldots; s_3]_{3I\times 1}$;
$B_1 = [Q_1; 0]_{7I\times I}$; $B_2 = [0; S_1]_{7I\times I}$; $B_3 = [Q_2; S_2]_{7I\times 2I}$;

$$B_4 = [Q_4 - Q_3A; S_3]_{7I\times 1};\ \overline{Q}_1 = \mathrm{diag}(q_1)_{4I\times I};\ \overline{Q}_3 = \mathrm{diag}(q_4)_{4I\times I};$$

$$\overline{Q}_4 = \begin{bmatrix} 0 & \dots & 0 & q_2 \\ 0 & \dots & q_2 & 0 \\ \dots & \dots & \dots & \dots \\ q_2 & \dots & 0 & 0 \end{bmatrix}_{4I\times I};\ \overline{Q}_5 = \begin{bmatrix} 0 & \dots & 0 & q_5 \\ 0 & \dots & q_5 & 0 \\ \dots & \dots & \dots & \dots \\ q_5 & \dots & 0 & 0 \end{bmatrix}_{4I\times I};$$

$$\overline{B}_1 = [\overline{Q}_1; 0]_{7I\times I};\ \overline{B}_2 = [0; S_1]_{7I\times I};\ \overline{B}_3 = [Q_2; S_2]_{7I\times 2I};$$

$$\overline{B}_4 = [Q_4 - \overline{Q}_3A - \overline{Q}_4\bar{t}_k - \overline{Q}_5\bar{A}; S_3]_{7I\times 1};$$

References

Ariano, A. D., Corman, F., Pacciarelli, D., & Pranzo, M. (2008). Reordering and Local Rerouting Strategies to Manage Train Traffic in Real. *Transportation Science, 42*(4), 405–419. https://doi.org/10.1287/trsc.1080.0247

Bärmann, A., Martin, A., & Schneider, O. (2021). Efficient Formulations and Decomposition Approaches for Power Peak Reduction in Railway Traffic via Timetabling. *Transportation Science, 55*(3), 747–767. https://doi.org/10.1287/trsc.2020.1021

Bemporad, A., & Morari, M. (1999). Control of systems integrating logic, dynamics, and constraints. *Automatica, 35*(3), 407–427. https://doi.org/10.1016/S0005-1098(98)00178-2

Breusegem, V. V., Campion, G., & Bastin, G. (1991). Traffic modeling and state feedback control for metro lines. *IEEE Transactions on Automatic Control, 36*(7), 770–784. https://doi.org/10.1109/9.85057

Campion, G., Van Breusegem, V., Pinson, P., & Bastin, G. (1985). Traffic regulation of an underground railway transportation system by state feedback. *Optimal Control Applications and Methods, 6*(4), 385–402. https://doi.org/10.1002/oca.4660060406

Chen, J. F., Lin, R. L., & Liu, Y. C. (2005). Optimization of an MRT train schedule: Reducing maximum traction power by using genetic algorithms. *IEEE Transactions on Power Systems, 20*(3), 1366–1372. https://doi.org/10.1109/TPWRS.2005.851939

Corman, F., D'Ariano, A., Pacciarelli, D., & Pranzo, M. (2010). A tabu search algorithm for rerouting trains during rail operations. *Transportation Research Part B: Methodological, 44*(1), 175–192. https://doi.org/10.1016/j.trb.2009.05.004

Corman, F., D'Ariano, A., Pacciarelli, D., & Pranzo, M. (2012). Bi-objective conflict detection and resolution in railway traffic management. *Transportation Research Part C: Emerging Technologies, 20*(1), 79–94. https://doi.org/10.1016/j.trc.2010.09.009

Ghasempour, T., & Heydecker, B. (2020). Adaptive railway traffic control using approximate dynamic programming. *Transportation Research Part C: Emerging Technologies, 113*, 91–107. https://doi.org/10.1016/j.trc.2019.04.002

Grube, P., & Cipriano, A. (2010). Comparison of simple and model predictive control strategies for the holding problem in a metro train system. *IET Intelligent Transport Systems, 4*(2), 161–175. https://doi.org/10.1049/iet-its.2009.0086

Hong, X., Meng, L., D'Ariano, A., Veelenturf, L. P., Long, S., & Corman, F. (2021). Integrated optimization of capacitated train rescheduling and passenger reassignment under disruptions. *Transportation Research Part C: Emerging Technologies, 125*, 103025. https://doi.org/10.1016/j.trc.2021.103025

Jin, B., Feng, X., Wang, Q., Sun, P., & Fang, Q. (2021). Train Scheduling Method to Reduce Substation Energy Consumption and Peak Power of Metro Transit Systems. *Transportation Research Record: Journal of the Transportation Research Board, 2675*(4), 201–212. https://doi.org/10.1177/0361198120974677

Li, S., Dessouky, M. M., Yang, L., & Gao, Z. (2017). Joint optimal train regulation and passenger flow control strategy for high-frequency metro lines. *Transportation Research Part B: Methodological, 99*, 113–137. https://doi.org/10.1016/j.trb.2017.01.010

Li, S., Li, S., Liu, R., Gao, Z., & Yang, L. (2021). Integrated train dwell time regulation and train speed profile generation for automatic train operations on high-density metro lines: A distributed optimal control method. *Transportation Research Part B, 148*, 82–105. https://doi.org/10.1016/j.trb.2021.04.009

Lin, W. S., & Sheu, J. W. (2011). Optimization of train regulation and energy usage of metro lines using an adaptive-optimal-control algorithm. *IEEE Transactions on Automation Science and Engineering, 8*(4), 855–864. https://doi.org/10.1109/TASE.2011.2160537

Li, W., Peng, Q., Wen, C., Wang, P., Lessan, J., & Xu, X. (2020). Joint optimization of delay-recovery and energy-saving in a metro system: A case study from China. *Energy, 202*, 117699. https://doi.org/10.1016/j.energy.2020.117699

Li, S., Yang, L., & Gao, Z. (2019). Efficient Real-Time Control Design for Automatic Train Regulation of Metro Loop Lines. *IEEE Transactions on Intelligent Transportation Systems, 20*(2), 485–496. https://doi.org/10.1109/TITS.2018.2815528

Moaveni, B., & Najafi, S. (2018). Metro traffic modeling and regulation in loop lines using a robust model predictive controller to improve passenger satisfaction. *IEEE Transactions on Control Systems Technology, 26*(5), 1541–1551. https://doi.org/10.1109/TCST.2017.2735945

Ning, J., Zhou, Y., Long, F., & Tao, X. (2018). A synergistic energy-efficient planning approach for urban rail transit operations. *Energy, 151*, 854–863. https://doi.org/10.1016/j.energy.2018.03.111

Novak, H., Lesic, V., & Vasak, M. (2018). Hierarchical Model Predictive Control for Coordinated Electric Railway Traction System Energy Management. *IEEE Transactions on Intelligent Transportation Systems, 20*(7), 2715–2727. https://doi.org/10.1109/TITS.2018.2882087

Pellegrini, P., Marlière, G., Pesenti, R., & Rodriguez, J. (2015). RECIFE-MILP: An Effective MILP-Based Heuristic for the Real-Time Railway Traffic Management Problem. *IEEE Transactions on Intelligent Transportation Systems, 16*(5), 2609–2619. https://doi.org/10.1109/TITS.2015.2414294

Pellegrini, P., Pesenti, R., & Rodriguez, J. (2019). Efficient train re-routing and rescheduling: Valid inequalities and reformulation of RECIFE-MILP. *Transportation Research Part B: Methodological, 120*, 33–48. https://doi.org/10.1016/j.trb.2018.12.008

Quaglietta, E., Corman, F., & Goverde, R. M. P. (2013). Stability analysis of railway dispatching plans in a stochastic and dynamic environment. *Journal of Rail Transport Planning & Management, 3*(4), 137–149. https://doi.org/10.1016/j.jrtpm.2013.10.009

Ramos, A., Pena, M. T., Fernandez, A., et al. (2007). Mathematical programming approach to underground timetabling problem for maximizing time synchronization. In *International Conference on Industrial Engineering and Industrial Management* (pp. 88–95).

Samà, M., D'Ariano, A., Corman, F., & Pacciarelli, D. (2017). A variable neighbourhood search for fast train scheduling and routing during disturbed railway traffic situations. *Computers and Operations Research, 78*, 480–499. https://doi.org/10.1016/j.cor.2016.02.008

Schön, C., & König, E. (2018). A stochastic dynamic programming approach for delay management of a single train line. *European Journal of Operational Research, 271*(2), 501–518. https://doi.org/10.1016/j.ejor.2018.05.031

Schwenzer, M., Ay, M., Bergs, T., & Abel, D. (2021). Review on model predictive control: An engineering perspective. *International Journal of Advanced Manufacturing Technology, 117*(5–6), 1327–1349. https://doi.org/10.1007/s00170-021-07682-3

Šemrov, D., Marsetič, R., Žura, M., Todorovski, L., & Srdic, A. (2016). Reinforcement learning approach for train rescheduling on a single-track railway. *Transportation Research Part B: Methodological, 86*, 250–267. https://doi.org/10.1016/j.trb.2016.01.004

Sheu, J. W., & Lin, W. S. (2012). Energy-saving automatic train regulation using dual heuristic programming. *IEEE Transactions on Vehicular Technology, 61*(4), 1503–1514. https://doi.org/10.1109/TVT.2012.2187225

Sirmatel, I. I., & Geroliminis, N. (2021). Stabilization of city-scale road traffic networks via macroscopic fundamental diagram-based model predictive perimeter control. *Control Engineering Practice, 109*, 104750. https://doi.org/10.1016/j.conengprac.2021.104750

Wang, X., Li, S., Su, S., & Tang, T. (2019). Robust Fuzzy Predictive Control for Automatic Train Regulation in High-frequency Metro Lines. *IEEE Transactions on Fuzzy Systems, 27*(6), 1295–1308. https://doi.org/10.1109/TFUZZ.2018.2877593

Wang, X., Li, S., Tang, T., & Yang, L. (2022). Event-Triggered Predictive Control for Automatic Train Regulation and Passenger Flow in Metro Rail Systems. *IEEE Transactions on Intelligent Transportation Systems, 23*(3), 1782–1795. https://doi.org/10.1109/tits.2020.3026755

Wang, Y., Zhao, K., D'Ariano, A., Niu, R., Li, S., & Luan, X. (2021). Real-time integrated train rescheduling and rolling stock circulation planning for a metro line under disruptions. *Transportation Research Part B: Methodological, 152*, 87–117. https://doi.org/10.1016/j.trb.2021.08.003

Wang, Z., Zha, J., & Wang, J. (2021). Autonomous Vehicle Trajectory Following: A Flatness Model Predictive Control Approach with Hardware-in-the-Loop Verification. *IEEE Transactions on Intelligent Transportation Systems, 22*(9), 5613–5623. https://doi.org/10.1109/TITS.2020.2987987

Wang, Y., Zhu, S., Li, S., Yang, L., & De Schutter, B. (2022). Hierarchical Model Predictive Control for on-Line High-Speed Railway Delay Management and Train Control in a Dynamic Operations Environment. *IEEE Transactions on Control Systems Technology*, 1–16. https://doi.org/10.1109/tcst.2022.3140805

Wu, N., Li, D., Xi, Y., & De Schutter, B. (2021). Distributed Event-Triggered Model Predictive Control for Urban Traffic Lights. *IEEE Transactions on Intelligent Transportation Systems, 22*(8), 4975–4985. https://doi.org/10.1109/TITS.2020.2981381

Yang, X., Li, X., Gao, Z., Wang, H., & Tang, T. (2013). A cooperative scheduling model for timetable optimization in subway systems. *IEEE Transactions on Intelligent Transportation Systems, 14*(1), 438–447. https://doi.org/10.1109/TITS.2012.2219620

Yin, J., Tang, T., Yang, L., Gao, Z., & Ran, B. (2016). Energy-efficient metro train rescheduling with uncertain time-variant passenger demands: An approximate dynamic programming approach. *Transportation Research Part B: Methodological, 91*, 178–210. https://doi.org/10.1016/j.trb.2016.05.009

Zhang, H., Li, S., Wang, Y., Wang, Y., & Yang, L. (2021). Real-time optimization strategy for single-track high-speed train rescheduling with disturbance uncertainties: A scenario-based chance-constrained model predictive control approach. *Computers and Operations Research, 127*, 105135. https://doi.org/10.1016/j.cor.2020.105135

Zhang, H., Li, S., & Yang, L. (2019). Real-time optimal train regulation design for metro lines with energy-saving. *Computers & Industrial Engineering, 127*, 1282–1296. https://doi.org/10.1016/j.cie.2018.02.019